

Optimization Methods in Geometric Shape Approximation

A THESIS
SUBMITTED TO THE FACULTY OF THE
UNIVERSITY OF MINNESOTA
BY

Mehdi Behroozi

IN PARTIAL FULFILLMENT OF THE REQUIREMENTS
FOR THE DEGREE OF
MASTER OF SCIENCE

Adviser: Dr. Gilad Lerman

August, 2021

© Mehdi Behrooz 2021
ALL RIGHTS RESERVED

Acknowledgements

During my academic journey towards this master's degree at the University of Minnesota, several events, most of them good, have happened that have delayed its completion until now. I ended up getting my Ph.D. in industrial engineering first and starting an academic career in the Mechanical and Industrial Engineering Department at Northeastern University before being able to turn my focus back on the completion of my M.S. in mathematics. To this end, I am first and foremost indebted to Professor Gilad Lerman for his extreme patience with my odd situation. My sincere appreciation also goes to him for all the things that I learned from him as a wonderful adviser, great mentor, and prominent scholar.

Throughout this research, I have also used the help and advice of Professors Shuzhong Zhang and John Gunnar Carlsson from the Department of Industrial and Systems Engineering, whose comments and key observations were extremely helpful in the derivation of some of the results.

I would also like to thank the thesis committee members, Professor Jeffrey Calder and Professor William Leeb, for being so responsive and accommodative in scheduling the defense and also for their valuable feedback and support.

I also appreciate the tremendous amount of effort that the faculty of the School of Mathematics at the University of Minnesota has put for me to teach me and elaborate me to a higher level of thoughtfulness and understanding. I certainly learned a lot from the stellar quality of courses at the School of Mathematics and via the outstanding research environment in its renowned research centers including, the Institute for Mathematics and Its Applications (IMA) and the Minnesota Center for Industrial Mathematics (MCIM).

The administration of the mathematics graduate program, in particular its director Professor Richard McGehee, and the staff members there, most notably Bonny Fleming, were extremely accommodative and helpful during my association with the program. My sincere gratitude goes to them. I must also thank my group-mates: Vahan Huroyan, Jeffery Moulton, Tyler Maunu, John Goes, Alex Gutierrez, Xu Wang, Mary Agwang, Nitin Prasad, Madeline Handschy, Yunpeng Shi, and James Rishabh Mishra, and other Math comrades in the School of Mathematics at the University of Minnesota for the stimulating discussions, and for all the fun we have had in the last few years. I appreciate the aid and support of all of my friends who have been with me during both happiness and hardship and made my time during these years more joyful and gave me a wonderful sense of exhilaration.

Last but not the least, I would like to express my deepest gratitude to my family whose unwavering love, unconditional support, and constant encouragement, throughout the ups and downs of my graduate studies, my academic career, and my entire life, in general, helped me to cope the difficulties and focus better towards this achievement.

Dedication

With the deepest feelings in my heart I dedicate this dissertation:

To,

My Parents,

who have held me dear over the years and I hold them dear forever!

Abstract

This thesis studies the application of optimization methods in approximating geometric shapes. In particular, it considers the problem of finding maximum volume (axis-aligned) inscribed parallelotopes and boxes in a compact convex set, defined by a finite number of convex inequalities, and presents an optimization approach for solving them. Several optimization models are developed that can be easily generalized to find other inscribed geometric shapes such as triangles, rhombi, and tetrahedrons. To find the largest axis-aligned inscribed rectangles in the higher dimensions, an interior-point method algorithm is presented and analyzed. Finally, a parametrized optimization approach is developed to find the largest (axis-aligned) inscribed rectangles in the two-dimensional space.

Contents

| | |
|--|------------|
| Acknowledgements | i |
| Dedication | iii |
| Abstract | iv |
| List of Figures | vii |
| 1 Introduction | 1 |
| 1.1 An Overview on Geometric Shape Approximation | 1 |
| 1.2 Contributions and Organization of the Thesis | 2 |
| 2 Preliminaries | 4 |
| 2.1 Notational Conventions | 4 |
| 2.2 Related work | 5 |
| 2.2.1 Geometric Shape Approximation | 5 |
| 2.2.2 Approximation with Rectangles | 5 |
| 2.2.3 MAAIR, MAIR, and Higher Dimensions | 6 |
| 3 Optimal Properties of the MAIR | 8 |
| 3.1 Optimal Properties of the MAIR in a Convex Polygon | 8 |
| 3.2 Optimal Properties of the MAIR in a Centrally Symmetric Convex Set . . . | 13 |
| 3.3 Optimal Properties of the MAIR in an Axially Symmetric Convex Set . . . | 14 |

| | | |
|----------|---|-----------|
| 4 | Optimization Models for MVIR and MVAIR | 20 |
| 4.1 | MVIR as an Optimization Problem | 20 |
| 4.2 | MVAIR as an Optimization Problem | 23 |
| 5 | Exact and Approximation Algorithms | 26 |
| 5.1 | Solving the MVAIR | 26 |
| 5.2 | Solving the MVIR | 35 |
| 6 | Computational Experiments | 48 |
| 6.1 | Simulation Results | 48 |
| 6.2 | Evaluation | 48 |
| 7 | Conclusion | 54 |
| | Bibliography | 55 |

List of Figures

| | | |
|-----|---|----|
| 1.1 | An inscribed box inside a convex set in 2D where the set C is a convex polygon. The inscribed rectangle R can be determined either by three vertices x^1, x^2, x^3 or by the vertex x^1 and the two vectors $u^1 = x^2 - x^1$ and $u^2 = x^3 - x^1$. The largest area inscribed rectangle is desired. | 2 |
| 3.1 | The illustration of the proof of the adjacency part in the second case (two vertex-corners) in Theorem 3. Rectangle R with one interior-corner which is diagonal to the vertex-corner. Figure (3.1a) shows the case when feasible directions exists as shown in Figure (3.1b) and Figure (3.1c) shows the case where there is no feasible direction for translation of R as seen in Figure (3.1d) but R can be rotated around corner d . The dashed rectangle shows the translated or rotated rectangle R' that has more than one interior-point. | 11 |
| 3.2 | The illustration of the proof of the third case (two vertex-corners) in Theorem 3. By constructing the angle $\hat{\theta}$ and then the new rectangle $R' = a'b'c'd'$, we can show that a non-square rectangle R with only two vertex-corners cannot be optimal. | 12 |
| 3.3 | An illustration of the proof of the Theorem 6. Rectangle R_s is the symmetric counterpart of R with respect to the center o and $R_t = R + \vec{x\bar{o}}$ is the translation of R in direction $\vec{x\bar{o}}$ and is centered at point $x_t = o$. Rectangle $R_t \subset \mathbf{Conv}(R, R_s) \subset C$ has the same size as R | 13 |

| | | |
|-----|--|----|
| 3.4 | An illustration of the proof of the first condition in Theorem 7. The line ℓ , is axis of symmetry of the convex set C with $\text{SymAxis}(C) = \ell \cap C$. Rectangle R lies on one side of ℓ and touches the boundary of C at three of its corners for which a tangent line of C at that point is drawn. The polygon P is the convex hull of R , $\text{SymAxis}(C)$, and the reflected image of R with respect to ℓ . The dashed rectangle shows R when translated in a feasible direction. . . | 15 |
| 3.5 | An illustration of the proof of the third condition in Theorem 7. Square R in Figure (3.5a) with three corner on one side of ℓ and a diagonal parallel to ℓ cannot be the MAIR as it can be translated in the direction orthogonal to ℓ leaving R with two interior-corners a, c and two edge- or interior-corners b, d . Figure (3.5b) shows the case where the diagonal of R is not aligned with ℓ . Since R is a square ℓ , the axis of symmetry, must lie within the slab defined by ℓ_1 and ℓ_3 , the bisectors of line segments $\overline{aa'}$ and $\overline{cc'}$ | 16 |
| 3.6 | An illustration of the proof of fourth condition in Theorem 7. Rectangle R has the $\text{SymAxis}(C)$ as its diagonal and has one vertex on the boundary of C on each side of the symmetry axis ℓ . The rectangle $R' = \square aa''cc''$ has a larger area than R | 17 |
| 5.1 | Sensitivity of the inscribed rectangles to the direction assuming a fixed vertex-corner. | 39 |
| 5.2 | An illustration of the proof of Lemma 19 for the upper bound on the aspect ratio of the MAIR in a convex set. The dashed rectangle is induced by the diameter of the set and the dotted rectangle is induced by the line segment that connects the touching points of the set and the shorter sides of its smallest axis-aligned bounding box. | 43 |
| 5.3 | An illustration of the proof of the lower bound in Lemma 20. The rectangle R' is the largest rectangle with direction $\theta^* + \alpha$ inscribed in R_{opt} and the rectangle R'' is induced by R' | 44 |

| | | |
|-----|---|----|
| 6.1 | The largest inscribed rectangle in two given polygons. The objective functions are shown in (6.1a) and (6.1c). It can be seen that $f(-1) = f(1)$ but $f(t)$ is not necessarily symmetric or even unimodal over $-1 \leq t \leq t$. The largest inscribed rectangles are obtained in (6.1b) and (6.1d), using the algorithm described in Section 5.2. “Poly vol.” shows the area (volume in general) of the polygon and “LIR vol.” show the area of the largest inscribed rectangle and the percentage of this area to the area of the polygon. Figure (6.1b) shows the MAIR with one vertex-corner and three edge-corners, while the MAIR in Figure (6.1d) has four edge-corners. | 50 |
| 6.2 | The largest inscribed rectangle in a random polygon with 14 vertices and a regular 500-gon randomly generated on a circle. The objective functions are shown in (6.2a) and (6.2c), which shows the contrast between a well-behaved unimodal quasiconvex and almost symmetric function and an ill-behaved non-smooth function. The largest inscribed rectangles are obtained in (6.2b) and (6.2d). It should be noted that the largest inscribed rectangle inside a circle is a square and the fraction of the area at optimality is $2/\pi \simeq 0.63662$ | 51 |
| 6.3 | The maximum area axis-aligned inscribe rectangles for the regular axes in a random 15-gon generated on a circle in (6.3a) and for two given directions in a given polygon in (6.3b). Note in Figure (6.3b) that the conditions of Theorem 3 may not hold for the maximum area rectangles for given directions as they may not be optimal regarding all directions. | 52 |
| 6.4 | The largest inscribed rectangles in two given ellipses. Notably, the fraction of the area of the MAIR to the area of the ellipse is the same as that of circles ($2/\pi \simeq 0.63662$), which can be verified by the elementary calculus. | 52 |
| 6.5 | The largest inscribed rectangle in the intersection of an ellipse and a parabola is presented in (6.5a) and for the intersection of an ellipse, a parabola, and a half-space is shown in (6.5b). We see that the conditions of the Theorem 3 hold for these particular non-polygonal examples. | 53 |

Chapter 1

Introduction

1.1 An Overview on Geometric Shape Approximation

In the context of Computational Geometry and Geometric Optimization, working with some geometric shapes, in the practical sense, is usually easier than others. For example, compare working with a regular polygon (equiangular and equilateral) versus a non-regular polygon, a simple polygon (not self-intersecting) vis-à-vis a self-intersecting polygon, a monotone polygon compared to a non-monotone polygon, or a convex polygon versus a non-convex polygon. Similarly, in many applications of geometric optimization, it is common to approximate the value of an objective function over a convex polygonal region with its value over a simpler approximating shape. Approximating a convex polygon with Löwner–John ellipsoids [1, 2, 3] or inner and outer boxes of Pólya and Szegő [4] are the prime examples of such approximations. This thesis studies the problem of approximating a convex set by its maximum volume inscribed rectangle. Figure 1.1 illustrates an instance of the problem in two-dimensional space (2D), where C is a convex polygon, R is an inscribed rectangle, and such rectangle with the largest area is desired. Practical applications of this kind of approximation arise in the apparel industry, footwear manufacturing, aluminum container production, steel/aluminum foil cutting, glass sheet cutting, sail manufacturing, carpet cutting, upholstery production, and many other industries. For example, in the apparel industry, the problem is to lay out small polygonal apparel pattern pieces in the unused

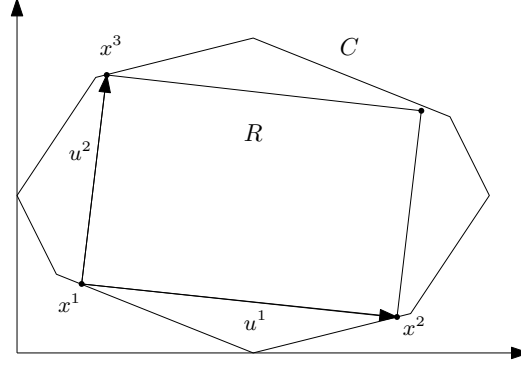


Figure 1.1: An inscribed box inside a convex set in 2D where the set C is a convex polygon. The inscribed rectangle R can be determined either by three vertices x^1, x^2, x^3 or by the vertex x^1 and the two vectors $u^1 = x^2 - x^1$ and $u^2 = x^3 - x^1$. The largest area inscribed rectangle is desired.

parts of a rectangular sheet of cloth, called “marker”, after laying out the larger pattern pieces to minimize waste [5, 6]. They compute the largest axis-aligned rectangle inside each trim piece (unused part) to work with a nicer geometric shape (see section 7 in [7]). In terms of application, the considered problem in this thesis is in the same spirit, but in a broader sense, of some other closely-related geometric optimization problems that include packing, covering, and tiling — generally focused on minimizing waste. These related problems include: cutting stock; knapsack; bin packing; guillotine; disk covering; polygon covering; kissing number; strip packing; square packing; squaring the square; squaring the plane; and, in three-dimensional space (3D), cubing the cube and tetrahedron packing.

1.2 Contributions and Organization of the Thesis

This thesis considers the problem of finding the largest parallelotopes and boxes inside a convex set defined by a finite number of convex inequalities. Throughout this thesis, for simplicity and due to the frequency of use, the term “rectangle” is used for all boxes $R \in \mathbb{R}^d$ and the term “Box” is reserved for cases with $d \geq 3$. We are interested in finding the *maximum volume/area inscribed parallelotope/parallelogram* (MVIP / MAIP), the *maximum volume/area inscribed rectangle* (MVIR / MAIR), and the *maximum volume/area axis-aligned inscribed rectangle* (MVAIR / MAAIR). The same acronyms are used for the

problem of finding them. The main contributions, listed in presentation order, are:

1. **Optimal properties of the MAIR in convex polygons** are discussed and proved (section 3.1). These properties are stronger and better formulated than the current results and yet with simpler proofs.
2. **Optimal properties of the MAIR in centrally symmetric and axially symmetric convex sets** are discussed and proved (section 3.2 and section 3.3). To the best of our knowledge this is first attempt in analyzing the properties of the MAIR in a convex set that is not necessarily a polygon.
3. **Optimization models for the MVIP, MVIR, and MVAIR problems** are developed (chapter 4). To our knowledge, this is the first comprehensive optimization approach to these problems in higher dimensions, which can bring new insights and open a new stream of research in this area. This approach is easily generalizable to other inscribed shapes such as triangles, rhombi, and tetrahedrons.
4. **An interior-point method algorithm** is used to solve the MVAIR problem (section 5.1). Full convergence analysis and computational complexity results are provided. To our knowledge, this is the first such algorithm and analysis that is presented for this problem.
5. **A parametrized optimization approach** is used to solve the MAAIR and the MAIR problems (section 5.2). To our knowledge, this is also the first parametrized optimization approach to solve these problems. Our algorithm for solving the MAAIR can solve the problem in any given direction, i.e., finding the largest rectangles aligned to rotated axes. When the convex set C is a polygon defined by n linear inequalities, this approach can find the MAIR in $\mathcal{O}(\varepsilon^{-1} \log n)$ time.
6. **An upper bound on the aspect ratio of the MAIR** in a convex set is derived, which is the first such result (section 5.2).
7. **Simulation results** are provided for several choices of the convex set (section 6.1).

Chapter 2

Preliminaries

2.1 Notational Conventions

Throughout this thesis, the following notational conventions are adopted: consider a compact convex set $C \in \mathbb{R}^d$. The boundary of C is shown with ∂C . The convex hull of a set of points p^1, \dots, p^n is shown by $\mathbf{Conv}(p^1, \dots, p^n)$. The line segment between points A and B is shown with \overline{AB} . The distance between two points p^1 and p^2 is shown by $\mathbf{dist}(p^1, p^2)$, while the distance between point p and a set S is defined as distance between p and its projection on S , i.e., $\mathbf{dist}(p, \mathbf{proj}(p, S))$. The diameter of $C \in \mathbb{R}^d$ is denoted by $\mathbf{diam}(C)$ and its volume by $\mathbf{Vol}(C)$. The area of $C \in \mathbb{R}^2$ is shown by $\mathbf{Area}(C)$. For simplicity of notation in proofs $|C|$ is also used to represent the volume (area) of C and similarly, $|\overline{AB}|$ is used to show the length of the line segment \overline{AB} . In 2D, a rectangle R with four corners at points A, B, C , and D is identified by $\square ABCD$ and a triangle with three corners at points A, B , and C is identified by $\triangle ABC$. The *aspect ratio* \mathbf{AR} of a rectangle $R \in \mathbb{R}^d$ with sides s_1, \dots, s_d is defined as the ratio of the length of its longest side to the length of its shortest side, i.e., $\mathbf{AR}(R) = \max_i s_i / \min_i s_i$. In 2D, this is $\mathbf{AR}(R) = \max \{height/width, width/height\}$, i.e., $\mathbf{AR} \geq 1$ and the equality holds for a square. We also define the aspect ratio of a non-rectangular convex set $C \subset \mathbb{R}^d$ as $\mathbf{AR}_{cvx}(C) = (\mathbf{diam}(C))^2 / \mathbf{Vol}(C)$. Finally, we denote by $\mathbf{refl}(\cdot, \ell)$ the reflected image of a point or a set under reflection at line ℓ and by $\mathbf{rot}(\cdot, o)$ the rotated image of a point or a set with respect to the center o .

2.2 Related work

2.2.1 Geometric Shape Approximation

The practice of approximating one geometric shape with another geometric shape is not restricted to approximating convex polygons with inscribed or circumscribing rectangles. DePano et al. [8] presented $\mathcal{O}(n^2)$ time algorithms for finding inscribed equilateral triangles and squares of maximum area inside convex polygons and an $\mathcal{O}(n^3)$ time algorithm for finding the largest inscribed equilateral triangle inside a general polygon, where with n is the number of vertices. Alt et al. [9] presented several polynomial time algorithms for the problem of approximating convex polygons with rectangles, circles, and polygons with fewer edges, where the approximate shape is not restricted to be inscribed or circumscribing but the area of its symmetric difference with the polygon or the Hausdorff distance of between their boundaries must be minimized. Zhu [10] expanded the results of [9] to three dimensional convex polyhedrons. Chaudhuri et al. [11] developed an $\mathcal{O}(n^3)$ time algorithm for the problem of finding the largest empty rectangle among a point set. Jin proposed an $\mathcal{O}(n^2)$ time algorithm [12] and an $\mathcal{O}(n \log^2 n)$ time algorithm [13] for finding all locally maximal area parallelograms inside a convex polygon. Recently, Keikha et al. [14] showed that a long-lasting linear-time algorithm for finding the maximal triangle inside a convex polygon proposed in 1979 by Dobkin and Snyder [15] was, in fact, incorrect and then provided an $\mathcal{O}(n \log n)$ time algorithm for this problem. However, there exist other linear-time algorithms for this problem proposed by Chandran and Mount [16], Kallus [17], and Jin [18].

2.2.2 Approximation with Rectangles

This thesis is primarily focused on approximation of convex polygons with rectangles. The history of the problem of approximating polygons with inscribed (circumscribed) rectangles goes back to the famous problem posed in 1951 by Pólya and Szegő [4, p. 110]. They showed that there exist homothetic rectangles R_1 and R_2 for a planar convex region C with the homothety ratio 3 such that $R_1 \subset C \subset R_2$. They also conjectured that the homothetic ratio

is no more than 2. Radziszewski [19] presented a lower bound on the area of the largest inscribed rectangle R inside a convex polygon C , as $\mathbf{Area}(R) \geq \frac{1}{2} \mathbf{Area}(C)$. Hadwiger [20] showed that for a convex body $C \subset \mathbb{R}^d$, there exist side-parallel d -dimensional rectangles R_1 and R_2 such that $R_1 \subset C \subset R_2$ and $\frac{1}{d!} \mathbf{Vol}(R_2) \leq \mathbf{Vol}(C) \leq d^d \mathbf{Vol}(R_1)$. Separately, Kosinski [21] proved that for a convex body $C \subset \mathbb{R}^d$, there exists a d -dimensional rectangle R such that $C \subset R$ and $\mathbf{Vol}(R) \leq d! \mathbf{Vol}(C)$. Grünbaum [22, pp. 258-259] showed that for a convex set $C \subset \mathbb{R}^2$ there exist parallelograms L_1 and L_2 such that $L_1 \subset C \subset L_2$ for which L_1 and L_2 are homothetic with the homothety ratio 2. Lassak [23] first proved Pólya and Szegő's conjecture and improved all the above results in 2D by showing that for any convex region $C \subset \mathbb{R}^2$ there are homothetic rectangles R_1 and R_2 for which R_1 is inscribed in C and R_2 is circumscribed about C with a positive homothety ratio of at most 2 and $\frac{1}{2} \mathbf{Area}(R_2) \leq \mathbf{Area}(C) \leq 2 \mathbf{Area}(R_1)$. Schwarzkopf *et al.* [24] obtained the same homothety ratio while presenting a more transparent proof. For a finer inner and outer approximation in 2D, Brinkhuis [25] showed that there exists a quadrangle Q that its sides support C at the vertices of a rectangle R_1 and at least three of its vertices lie on the boundary of a rectangle R_2 that is a dilation of R_1 with ratio 2.

2.2.3 MAAIR, MAIR, and Higher Dimensions

Amenta [26] proposed a convex programming model with exponential number of constraints to find the d -dimensional MVAIR inside the intersection of a family of n convex sets in d -dimensional space. In 2D, Daniels et al. [7, 27] proposed an $\mathcal{O}(n\alpha(n) \log^2 n)$ time algorithm for finding the MAAIR inside an n -vertex horizontally (vertically) convex polygon, where $\alpha(n)$ is the slowly growing inverse of Ackermann function [28]. For orthogonally convex polygons the algorithm performs in $\mathcal{O}(n\alpha(n))$ time. Fischer and Höffgen [29] developed an exact $\mathcal{O}(\log^2 n)$ time algorithm to compute the MAAIR in a convex n -gon. Alt et al. [30] developed an exact $\mathcal{O}(\log n)$ time algorithm for the same problem.

For MAIR, Hall-Holt et al. [31] developed a polynomial-time approximation scheme (PTAS), which for any fixed $\varepsilon > 0$ computes the $(1 - \varepsilon)$ -approximation to the optimal solution of the maximum area c -fat rectangle, i.e. a rectangle with aspect ratio bounded

by c , inside a “simple” polygon in $\mathcal{O}(n)$ time. Knauer et al. [32] showed that the fatness condition is unnecessary for approximating the optimal MAIR when the input polygon is convex. They developed a randomized $\mathcal{O}(\varepsilon^{-1} \log n)$ time ε -approximation algorithm that works with probability t for any constant $t < 1$ and a deterministic $\mathcal{O}(\varepsilon^{-2} \log n)$ time ε -approximation algorithm. Their algorithm uses Alt et al.’s exact algorithm [30] for finding MAAIR as a subroutine. It appears that the analysis of the running time of this algorithm misses the fact that for using Alt et al.’s algorithm [30] to find the MAAIR aligned to the ε -direction of the MAIR, one needs to rotate the axes or the polygon to that direction, which takes $\mathcal{O}(n)$ time (to make this a fair comparison we consider this part as pre-processing in one of our algorithms). This algorithm was the first ε -approximation algorithm for finding the MAIR inside a convex polygon. They have also sketched a straightforward exact algorithm that works in $\mathcal{O}(n^4)$ time. Finally, Cabello et al. [33] presented an $\mathcal{O}(n^3)$ exact algorithm and also an ε -approximation algorithm for this problem. Their approximation algorithm works for any convex set in running time $\mathcal{O}(\varepsilon^{-3/2} + \varepsilon^{-1/2} T_C)$, where T_C is the time needed to perform two different queries on C due to [34]. For a convex polygon, whose vertices are given as a sorted array or as a binary search tree, those queries can be done in $\mathcal{O}(\log n)$ time.

Chapter 3

Optimal Properties of the MAIR

3.1 Optimal Properties of the MAIR in a Convex Polygon

To understand the optimal inscribed rectangles better and before diving into the optimization models and algorithms in higher dimensions, we begin with the geometric properties of the traditional largest inscribed rectangles in a convex polygon in 2D. This section discusses the optimal properties of the MAIR in a convex polygon $C \subset \mathbb{R}^2$.

DePano et al. [8] proved that a maximum area equilateral triangle inscribed in C must have at least one corner coincident with a vertex of C . They also proved that a maximum area square inscribed in C either has at least one corner coincident with a vertex of C , or all four corners lie on the interior of edges of C . Schwarzkopf et al. [24] showed that the maximum area rectangle inscribed in C has two diagonal vertices lie on the boundary of C . Knauer et al. [32] mentioned without proof that the largest inscribed rectangle inside C is either a square with two opposite corners coincident with two vertices of C or has at least three non-vertex corners on the boundary of C . The latter statement seems to be incorrect or a misstatement. Schlipf [35] proved the former statement of [32] and also proved that a rectangle with three non-vertex corners on the boundary of C cannot be optimal. We strengthen these results and provide a much simpler proof.

Observation 1. *Consider a family of axis-aligned rectangles in \mathbb{R}^2 with a diagonal of fixed size ℓ that makes angle θ with the x -axis with $0 \leq \theta \leq \pi/4$. Among all such rectangles*

generated by this diagonal, the rectangle with $\theta = \pi/4$ has the largest area. Similarly, for rectangles with $\pi/4 \leq \theta \leq \pi/2$ the area is maximized when $\theta = \pi/4$. In other words, the square has the maximum area among the rectangles of the same diagonal size.

Definition 2. A corner of an inscribed rectangle inside C is one of the following types:

- (a) A *vertex-corner* which coincides with a vertex of C .
- (b) An *edge-corner* which lies on a non-vertex point of an edge (boundary) of C .
- (c) An *interior-corner* which lies strictly inside C .

Theorem 3. The MAIR inside a convex polygon C must satisfy at least one of the following conditions:

Case 1: It has no interior-corner (i.e., the four corners are on ∂C).

Case 2: It has one interior-corner and at least one vertex-corner adjacent to the interior-corner.

Case 3: It has two diagonal interior-corners, two diagonal vertex-corners, and the MAIR is a square.

Proof. Consider an inscribed rectangle R with vertices a, b, c and d in a c.c.w. order and dimensions $w \times h$. We prove by contradiction that if none of the conditions hold for R , it cannot be the MAIR and that in each of these three cases the specified conditions must hold. The cases in the theorem are organized based on the number of interior-corners of the rectangle. So we present the proof in the same organized manner.

If R has four or three interior-corners, we can easily expand both its length and width. This rules out all cases not specified in the theorem. If R has no interior-corner (Case 1), it is easy to see examples for which the MAIR can have four edge-corners. For example, if C is a triangle there is a MAIR satisfying this condition.

If R has one interior-corner (Case 2) and no vertex-corner, say three edge-corners a, b and c lying on edges e_a, e_b and e_c . Let l_a be the perpendicular line to e_a at a . Similarly define l_b and l_c for b and c . Let p_1 be the intersection of l_a and l_b and p_2 be the intersection of l_b and l_c . A small rotation of C in either directions around p_1 (or p_2), will put a, b

(or b, c) in the interior of C . At least one of these rotations (c.w. or c.c.w) will do the same for c (or a). Hence, R cannot be the MAIR. This proves that if the MAIR has one interior point it should have at least one vertex point as this rotation argument would not hold for a vertex-corner. It remains to prove that this vertex-corner should be adjacent to the interior-corner. Assume they are diagonal to each other. Without loss of generality (w.l.o.g.) let a the lower left corner of R be the vertex-corner and c be the interior-corner; see Figure 3.1. If either b or d is a vertex corner the case is proved. So let b and d be both edge-corners. Let e_a^1 and e_a^2 denote the edges of C at the vertex a such that e_a^1 lies below R and e_a^2 lies to the left of R . Also, let e_b and e_d be edges of C tangent to the corners b and d , respectively. Let K_a be a cone of directions (vectors) created by the directions of e_a^1 and e_a^2 . By convexity of C and perpendicularity of the edge of R , the directions of e_b and e_d must lie inside K_a . If the angle between e_d and e_a^1 is greater than (or equal to) the angle between e_b and e_a^1 , then a small enough translation of R in the direction of e_b , will keep b on e_b , will keep c an interior-corner, will make d an interior-corner (or slide it along the edge e_d , and will make a an interior-corner. This means R cannot be the MAIR. It is crucial to note that the translation could be done with respect to any direction that lies between the direction of e_b and e_d in the cone K_a . If the angle between e_d and e_a^1 is smaller than the angle between e_b and e_a^1 , there will be no feasible direction of translation. However, in this case R can be rotated around d in a c.c.w direction, putting both a and b strictly inside C while keeping c as an interior-corner. This rotation is possible since c is an interior-corner. This proves Case 2.

If R has two interior-corners (Case 3) that are adjacent to each other, then we can expand R in the direction perpendicular to the edge connecting these two corners. If R has two diagonal interior-corners, say b and d , and two edge-corners, say a and c , touching edges e_a and e_c , rotating C slightly around a (or c) either c.w. or c.c.w. will put c (or a) and maintain b and d strictly inside the polygon and hence we can enlarge it. The direction of rotation (c.w or c.c.w.) is toward increasing the obtuse angle between the diagonal \overline{ac} and e_c (or \overline{ac} and e_a). If it is a right angle then both directions work. If R has two diagonal interior-corners and there is just one vertex-corner, a slight rotation of C around

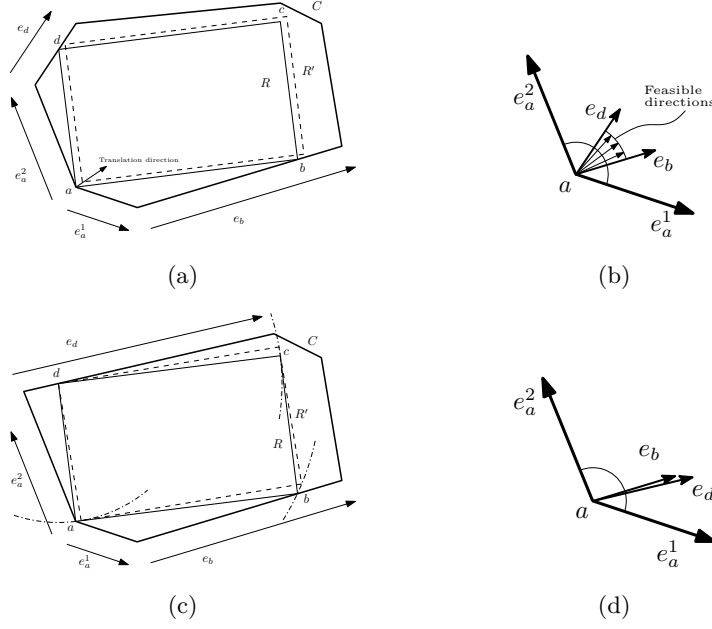


Figure 3.1: The illustration of the proof of the adjacency part in the second case (two vertex-corners) in Theorem 3. Rectangle R with one interior-corner which is diagonal to the vertex-corner. Figure (3.1a) shows the case when feasible directions exists as shown in Figure (3.1b) and Figure (3.1c) shows the case where there is no feasible direction for translation of R as seen in Figure (3.1d) but R can be rotated around corner d . The dashed rectangle shows the translated or rotated rectangle R' that has more than one interior-point.

the vertex-corner will put the fourth corner, which is an edge-corner, and keep the two interior-corners strictly inside C and hence makes it expandable. This proves that if R has two interior corners they should be diagonal and the other two vertices should be diagonal vertex-corners

If R has two diagonal interior-corners, say b and d , and two vertex-corners, say a and c , but it is not a square, the proof is a little more complicated. Let $\theta = \angle bac$; see Figure 3.2. Let θ_1 be the maximum angle for c.w. rotation of R around a such that b stays in C . Similarly θ_2 be the maximum angle for c.w. rotation of R around c such that d stays in C . Since R is not a square, we have either $w > h$ or $w < h$. Without loss of generality assume $w > h$ and thus $\theta = \arctan(h/w) < \pi/4$. Choose $\hat{\theta} > 0$ such that $\hat{\theta} < \min\{(\frac{\pi}{4} - \theta), \theta_1, \theta_2\}$. Notice that if R is a square we cannot find such $\hat{\theta}$. Now without loss of generality assume $\theta_1 < \theta_2$. Rotate R , c.w. around a as much as angle $\hat{\theta}$. Let $\hat{R} = \hat{a}\hat{b}\hat{c}\hat{d}$ denote the rotated

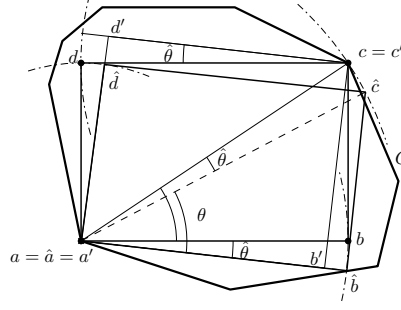


Figure 3.2: The illustration of the proof of the third case (two vertex-corners) in Theorem 3. By constructing the angle $\hat{\theta}$ and then the new rectangle $R' = a'b'c'd'$, we can show that a non-square rectangle R with only two vertex-corners cannot be optimal.

rectangle. Then clearly $a = \hat{a}$, \hat{b} lies either strictly inside or on an edge of C , \hat{c} is possibly outside C , and \hat{d} is inside C . Rotate the segment \overline{cd} in a c.w. direction as much as angle $\hat{\theta}$. The whole rotated segment, call it r_{cd} , will stay inside C . Extend $\overline{\hat{a}\hat{d}}$ to touch r_{cd} . Call the intersection point d' and let $a' = a$. It can be seen that $\overline{a'd'}$ is perpendicular to r_{cd} . Draw a line from c parallel to $\overline{a'd'}$ to touch $\overline{\hat{a}\hat{b}}$ at b' and let $c' = c$. It can also be observed that $\overline{b'c'}$ is perpendicular to $\overline{a'b'}$. Then the new rectangle $R' = \square a'b'c'd'$ is inscribed inside C , has two diagonal vertex-corners, has the same diagonal as R , and the $\angle b'a'c'$ is greater than θ . Therefore, we have $\mathbf{Area}(R') > \mathbf{Area}(R)$ by Observation 1. This proves Case 3.

Finally, none of the three conditions in the theorem is redundant since for each one of them we can easily construct a polygon that gives us a MAIR satisfying that condition. \square

The following corollaries are direct results of Theorem 3.

Corollary 4. *The MAIR has at least two diagonal corners on the boundary of C . Unless both of these corners are vertex-corners at least one other corner has to lie on ∂C .*

Corollary 5. *Each interior corner, if any exists, has two adjacent corners on the boundary of C .*

3.2 Optimal Properties of the MAIR in a Centrally Symmetric Convex Set

The following theorem summarizes a basic property of the MAIR in a centrally symmetric convex set.

Theorem 6. *Let C be a centrally symmetric convex compact set with respect to the center o and let R_{opt} be the MAIR inside C . Then, the center of R_{opt} , i.e., the intersection of its diagonals, must lie at o .*

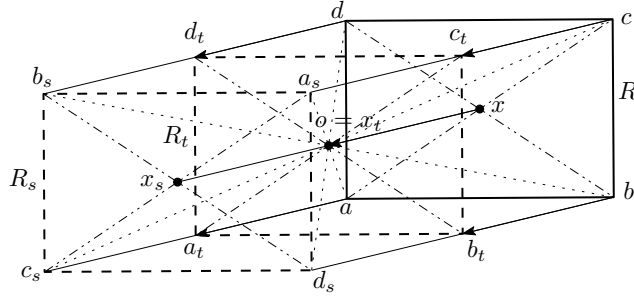


Figure 3.3: An illustration of the proof of the Theorem 6. Rectangle R_s is the symmetric counterpart of R with respect to the center o and $R_t = R + \vec{x}\vec{o}$ is the translation of R in direction $\vec{x}\vec{o}$ and is centered at point $x_t = o$. Rectangle $R_t \subset \mathbf{Conv}(R, R_s) \subset C$ has the same size as R .

Proof. Consider $R \square abcd \subset C$ with its center at a point $x \neq o$. We first prove that the direction $\vec{x}\vec{o}$ is a feasible translation direction for R and for any such rectangle there exists a rectangle with the same size centered at o . Since C is centrally symmetric with respect to x , let $R_s = \square a_s b_s c_s d_s \subset C$ be the symmetric counterpart of R with respect to the center o , as shown in Figure 3.3. We must have $\overline{ac} \parallel \overline{a_s c_s}$ and $\overline{bd} \parallel \overline{b_s d_s}$ with $|\overline{ac}| = |\overline{a_s c_s}| = |\overline{bd}| = |\overline{b_s d_s}|$. Therefore, we have $\overline{xx_s} \parallel \overline{ac_s} \parallel \overline{ca_s} \parallel \overline{bd_s} \parallel \overline{db_s}$, and $|\overline{xx_s}| = |\overline{ac_s}| = |\overline{ca_s}| = |\overline{bd_s}| = |\overline{db_s}|$. Let R_t be the rectangle that has its center at $x_t = o = (x + x_s)/2$ and its corners a_t, b_t, c_t, d_t at the midpoint of segments $\overline{ac_s}, \overline{bd_s}, \overline{ca_s}, \overline{db_s}$, respectively. Note that $R_t \subset \mathbf{Conv}(R, R_s) \subset C$, $|R_t| = |R|$, and R_t is a translation of R in direction $\vec{x}\vec{o}$.

Now, if \overline{ox} is aligned with an edge of R then $R' = \mathbf{Conv}(R, R_s)$ is a rectangle and $|R'| > |R|$, since $x \neq o$. If \overline{ox} is not aligned with an edge of R , then $\mathbf{Conv}(R, R_s)$ is an irregular hexagon in which R has one interior-corner, assume w.l.o.g. that this is corner a ,

and three vertex-corners. Translating R slightly in the direction $\vec{x\bar{o}}$ will keep a as interior-corner but makes b, c, d edge-corners. Therefore, by theorem 3, R cannot be the MAIR. \square

3.3 Optimal Properties of the MAIR in an Axially Symmetric Convex Set

The following theorem summarizes some of the properties of the MAIR in an axially symmetric convex set.

Theorem 7. *Let C be an axially symmetric convex compact set, ℓ be its line of axial symmetry with $\text{SymAxis}(C) = \ell \cap C$, and R_{opt} be the MAIR inside C . Then, R_{opt} must satisfy the following conditions:*

1. *We must have $\Lambda = \ell \cap R_{\text{opt}} \neq \emptyset$, and the set Λ is not a singleton or an edge of R_{opt} .*
2. *Unless R_{opt} has a corner on one end point of $\text{SymAxis}(C)$, at least one corner of R_{opt} must lie on ∂C in each side of ℓ .*
3. *If R_{opt} is a square it cannot have three corners strictly on one side of ℓ .*
4. *If R_{opt} has two corners (a diagonal) on $\text{SymAxis}(C)$, it is either a square or a rectangle that makes an angle $\pi/6 \leq \alpha < \pi/4$ with ℓ .*

Proof. We first prove the intersection condition. Consider rectangle $R \subset C$ and assume $R = R_{\text{opt}}$ and that $\Lambda = \ell \cap R$ is an empty set, a singleton, or an edge of R . Under any of these three conditions, we must have R completely on one side of ℓ . Assume, w.l.o.g., that ℓ is aligned with the x -axis and consider rectangle $R = \square abcd \subset C$, in c.c.w. order with a being the lower left corner, lies above ℓ as shown in Figure 3.4. Let the points a', b', c', d' be the reflection of corners a, b, c, d with respect to ℓ . In other words, $R'_\ell = \square a'b'c'd' = \text{refl}(R, \ell) \subset C$ is the reflection of R at ℓ and has the same size as R . Also let p, q be the left and right end of $\text{SymAxis}(C)$ and define the polygon $P = \mathbf{Conv}(p, q, a, b, c, d, a', b', c', d')$. Note that $P \subset C$ and $|\text{SymAxis}(C)| = |\overline{pq}| \geq |\overline{bd}| = |\overline{a'c}|$. If R has four corners on ∂C then R must be aligned to ℓ , due to the convexity of C , P must be a rectangle, and R can be

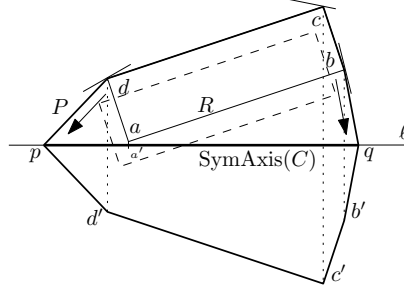


Figure 3.4: An illustration of the proof of the first condition in Theorem 7. The line ℓ , is axis of symmetry of the convex set C with $\text{SymAxis}(C) = \ell \cap C$. Rectangle R lies on one side of ℓ and touches the boundary of C at three of its corners for which a tangent line of C at that point is drawn. The polygon P is the convex hull of R , $\text{SymAxis}(C)$, and the reflected image of R with respect to ℓ . The dashed rectangle shows R when translated in a feasible direction.

extended in the direction orthogonal to ℓ due to the axial symmetry of C , contradicting the assumption. If only two corners of R touch ∂C , then R can be easily enlarged by either extension (if these two corners are adjacent) or first rotation and then extension (if these two corners are diagonal by rotating around one of these two corners that has a larger distance to ℓ). Hence, R must have three of its corners on ∂C and must have an angle with ℓ , making either a or b an interior-corner. Let a be the interior-corner (w.l.o.g.). Due to the axial symmetry and convexity of C , the vectors \vec{dp} and \vec{bq} must be either parallel or diverging. Any direction within the cone defined by these two vectors would be a translation direction that could put at least one more corner of R in the interior of C . Therefore, $R \neq R_{opt}$. Note that in this case and the other two corners that are still potentially on ∂C would be either interior-corners or edge-corners on ∂P , which also shows by Theorem 3 that R cannot be the MAIR. If the set Λ is a singleton, it must be an interior-corner of R , e.g., a , and the same translation argument applies. If Λ is equal to an edge of R then R is aligned to ℓ and it can be extended in the direction orthogonal to ℓ . This proves that line ℓ crosses ∂R_{opt} in two points, i.e., $\ell \cap \text{int } R_{opt} \neq \emptyset$ (1st condition).

For the second condition), by the intersection condition, we know that at least one corner of R_{opt} lies on each side of ℓ . If R_{opt} has no corner on the endpoints of $\text{SymAxis}(C)$, we must have at least one corner of R_{opt} on ∂C in each side of ℓ , otherwise the translation and extension are possible and R_{opt} could be enlarged.

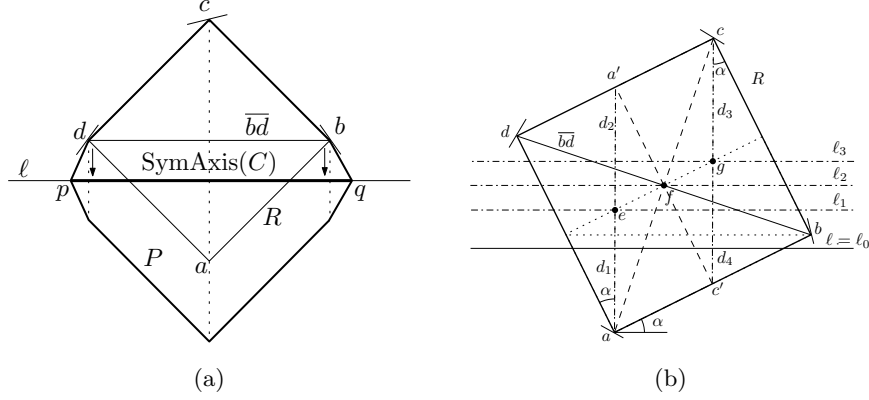


Figure 3.5: An illustration of the proof of the third condition in Theorem 7. Square R in Figure (3.5a) with three corner on one side of ℓ and a diagonal parallel to ℓ cannot be the MAIR as it can be translated in the direction orthogonal to ℓ leaving R with two interior-corners a, c and two edge- or interior-corners b, d . Figure (3.5b) shows the case where the diagonal of R is not aligned with ℓ . Since R is a square ℓ , the axis of symmetry, must lie within the slab defined by ℓ_1 and ℓ_3 , the bisectors of line segments $\overline{aa'}$ and $\overline{cc'}$.

Now we prove that if R_{opt} is a square, it cannot have three corners “strictly” on one side of ℓ . Assume ℓ crosses the boundary of square $R \subset C$ in two points and that R has three corners strictly on one side of ℓ and the last corner strictly on the other side of ℓ . Then R must have an angle α with ℓ . Without loss of generality assume a is the corner of R below ℓ and let $P = \mathbf{Conv}(p, q, R, \text{refl}(R, \ell))$. If R has three corners on one side of ℓ and its diagonal \overline{bd} is parallel to the line ℓ , then a cannot be on the ∂C , contradicting the second condition; see Figure (3.5a). In this case, a small enough translation of R in the orthogonal direction to ℓ would make c in interior-corner while keeping a in the interior of the polygon $P \subset C$. The corners b and d would be either interior-corners or edge-corners with respect to the polygon P . Hence, by Theorem 3, R cannot be the R_{opt} inside P and therefore cannot be the MAIR in C .

Now assume R is a square that has three corners on one side of ℓ and makes angle $0 < \alpha < \pi/4$ with ℓ , i.e., its diagonal \overline{bd} is not parallel to ℓ ; see Figure (3.5b). Let a' and c' be the points that vertical lines (perpendicular to ℓ) going through a and c intersect the edges \overline{cd} and \overline{ab} , respectively. Clearly, the quadrangle $aa'cc'$ is a parallelogram. Let ℓ_1, ℓ_2 and ℓ_3 be lines parallel to $\ell = \ell_0$ such that ℓ_1 bisects $\overline{aa'}$ at the point e , ℓ_2 goes through the center point f of the parallelogram, and ℓ_3 bisects $\overline{cc'}$ at the point g . The line

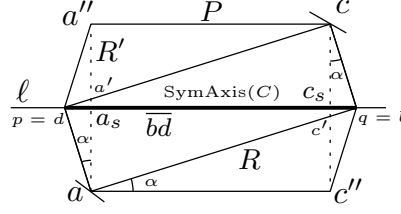


Figure 3.6: An illustration of the proof of fourth condition in Theorem 7. Rectangle R has the $\text{SymAxis}(C)$ as its diagonal and has one vertex on the boundary of C on each side of the symmetry axis ℓ . The rectangle $R' = \square aa''cc''$ has a larger area than R .

ℓ_i , $i = 0, 1, 2, 3$ partitions the segment $\overline{aa'}$ into two pieces with lengths d_1^i in the bottom and d_2^i at the top and the segment $\overline{cc'}$ into two pieces with lengths d_3^i on the top and d_4^i in the bottom. Obviously, $d_1^i + d_2^i = d_3^i + d_4^i$, $\forall i$. For ℓ_1 , we have $d_1^1 = d_2^1$ and $d_3^1 > d_4^1$. For ℓ_3 , we have $d_1^3 > d_2^3$ and $d_3^3 = d_4^3$. In the case of ℓ_2 , we have $d_1^2 = d_3^2 > d_2^2 = d_4^2$. Note that since the diagonal \overline{bd} is not parallel to ℓ , the lines ℓ_1, ℓ_2 and ℓ_3 are distinguished, otherwise the three lines would coincide with \overline{bd} . Also, by Thales's basic proportionality theorem, the bisector of edges \overline{ad} and \overline{bc} goes through the points e, f and g . Since R is a square we can show that all three lines will cross \overline{ad} and \overline{bc} and thus have two corners of R on each side. For ℓ_1 not crossing \overline{bc} , we must have $d_1^1 < |\overline{ab}| \sin \alpha$, while we have the opposite as $d_1^1 = d_2^1 = |\overline{aa'}|/2 = |\overline{ad}|/(2 \cos \alpha) = |\overline{ab}|/(2 \cos \alpha) > |\overline{ab}| \sin \alpha$, as we have $2 \sin \alpha \cos \alpha = \sin 2\alpha < 1$ for $0 < \alpha < \pi/4$. The proof for ℓ_3 is symmetric. By the second condition we must have $a \in \partial C$ (otherwise, R could be shifted in the direction orthogonal to ℓ , making c an interior-corner). Therefore, we must have $d_1^0 \geq d_2^0$ and $d_3^0 \geq d_4^0$ due to the convexity and axial symmetry of C . Hence ℓ must lie in the slab defined by ℓ_1 and ℓ_3 contradicting the assumption of having three corners on one side. This concludes the proof of the third condition.

We prove the fourth condition by first showing by construction that such a square exists and then we prove that the same does not hold for a rectangle with $0 < \alpha < \pi/6$. Consider a square $R = \square abcd$ with its diagonal \overline{bd} aligned to the x -axis. Let C be the rhombus obtained by stretching R slightly by extending the diagonal \overline{bd} for some $\delta > 0$. For sufficiently small δ , the square R would be the MAIR inside C with its diagonal on the $\text{SymAxis}(C)$ and one vertex-corner on the boundary of polygon C on each side of the symmetry axis.

We now prove that a rectangle $R = \square abcd$ that has its diagonal on the $\text{SymAxis}(C)$ and makes angle $0 < \alpha < \pi/6$ with ℓ cannot be the MAIR. Assume the most restrictive case where the diagonal \overline{bd} is equal to the $\text{SymAxis}(C)$ and $a, c \in \partial C$; see Figure 3.6. Let a_s, a' , and a'' be the points that a vertical line going through the corner a crosses the $\text{SymAxis}(C)$, the edge cd , and ∂C on the opposite side of ℓ , respectively. Similarly define the points c_s, c' , and c'' . Due to the symmetry of C with respect to ℓ and the fact that $a, c \in \partial C$ we must have $\mathbf{dist}(a'', a_s) = \mathbf{dist}(a, a_s) \geq \mathbf{dist}(a_s, a')$ and $\mathbf{dist}(c'', c_s) = \mathbf{dist}(c, c_s) \geq \mathbf{dist}(c_s, c')$. We prove that the rectangle $R' = \square aa''cc''$ satisfies $|R'| > |R|$, when $0 < \alpha < \pi/6$. As R' is aligned with ℓ , we have

$$|R'| = |\overline{ac''}| \times |\overline{aa''}| = (|\overline{ab}| - |\overline{ad}| \tan \alpha) \cos \alpha \times 2|\overline{ad}| \cos \alpha = 2|\overline{ab}| \times |\overline{ad}| \cos^2 \alpha - 2|\overline{ad}|^2 \sin \alpha \cos \alpha$$

Therefore,

$$\frac{|R'|}{|R|} = \frac{2|\overline{ab}| \times |\overline{ad}| \cos^2 \alpha - 2|\overline{ab}| \times |\overline{ad}| \tan \alpha \sin \alpha \cos \alpha}{|\overline{ab}| \times |\overline{ad}|} = 2(\cos^2 \alpha - \sin^2 \alpha) = 2 \cos 2\alpha \geq 1, \text{ for } 0 < \alpha < \pi/6$$

This concludes the proof of fourth condition. \square

Observation 8. *If a compact convex set $C \in \mathbb{R}^2$ has two perpendicular axes of symmetry ℓ_1 and ℓ_2 that cross each other at point o , then it is centrally symmetric with respect to the center o , as a rotation with angle π of any point $p \in C$ is achieved by two consecutive reflections with respect to lines ℓ_1 and ℓ_2 , i.e., $\text{rot}(p, \pi) = \text{refl}(\text{refl}(p, \ell_1), \ell_2)$ and we will have $\text{rot}(p, \pi) \in C$. This can be also be seen by the fact that $(p+p')/2 = (p+(-p+2o))/2 = o$.*

Observation 9. *In a compact convex set $C \in \mathbb{R}^2$ that is centrally symmetric with respect to a center o , the $\text{diam}(C)$ goes through o . Furthermore, if C has two perpendicular axes of symmetry, the $\text{diam}(C)$ may not be necessarily aligned to the axes of symmetry.*

Corollary 10. *Let C be an axially symmetric convex compact set with two perpendicular axes of symmetry ℓ_1 and ℓ_2 and let R_{opt} be the MAIR inside C . Also, assume the quadrants created by the intersection of ℓ_1 and ℓ_2 are numbered from 1 to 4 in a c.c.w order starting*

from top right quadrant and let $SymAxis_1(C) = \ell_1 \cap C$ and $SymAxis_2(C) = \ell_2 \cap C$. Then, R_{opt} must satisfy the following conditions:

1. The center of R_{opt} , i.e., the intersection of its diagonals, must lie at the intersection of ℓ_1 and ℓ_2 .
2. Unless R_{opt} has a corner on one end point of $SymAxis_1(C)$ or $SymAxis_2(C)$, at least one corner of R_{opt} must lie on ∂C in each side of ℓ_1 and ℓ_2 .
3. If R_{opt} is a square it either has its diagonals on $SymAxis_1(C)$ and $SymAxis_2(C)$ or has one corner strictly in each quadrant. It must also have at least two diagonally opposite corners on ∂C .
4. If R_{opt} has two corners (a diagonal) on $SymAxis_i(C)$, $i = 1, 2$, it is either a square or a rectangle that makes an angle $\pi/6 \leq \alpha < \pi/4$ with ℓ_i .

Proof. The first condition is proved by Observation 8 and Theorem 6. The second condition is a direct application of the 2nd condition in Theorem 7 to both ℓ_1 and ℓ_2 . The third condition follows from applying 2nd, 3rd, and 4th conditions in Theorem 7 to both ℓ_1 and ℓ_2 . The fourth condition also follows from the 4th conditions in Theorem 7. \square

Chapter 4

Optimization Models for MVIR and MVAIR

Consider a compact convex set $C \in \mathbb{R}^d$ mathematically expressible in a finite number of convex inequalities. For example, one could consider C to be a polytope defined by $C = \{x \in \mathbb{R}^d \mid Px \leq b, P \in \mathbb{R}^{n \times d}, b \in \mathbb{R}^n\}$ or intersection of d -ellipsoids defined as $C = \{x \in \mathbb{R}^d \mid x^T A_i x + 2b_i^T x + c_i \leq 0, i = 1, \dots, n\}$. The goal is to formulate the problems of finding the MVIR and the MVAIR inside C as optimization problems.

4.1 MVIR as an Optimization Problem

To make the derivation of the optimization model for the MVIR more clear, first, let's consider the d -dimensional maximum volume inscribed parallelotope in C . Let x^1, x^2, \dots, x^{d+1} be a set of $d+1$ affinely independent vertices of the parallelotope and put $U = [u^1 \ u^2 \ \dots \ u^d]$, where $u^i = x^{i+1} - x^1, i = 1, \dots, d$. Note that columns of U are linearly independent and form a basis for \mathbb{R}^d . See Figure 1.1 for an instance in 2D, where C is a polygon and the desired parallelogram is a rectangle.

The following definitions are required for constructing the optimization model.

Definition 11. A vector $x = (x_1, \dots, x_d)$ in \mathbb{R}^d is lexicographically positive if its first non-zero coordinate is positive.

Definition 12. Two points $x, y \in \mathbb{R}^d$ are in lexicographic order if $y - x$ is lexicographically positive.

Let's label the 2^d vertices of the parallelotope in a lexicographic order with binary vectors so that $q^1 = (0, \dots, 0)^T \equiv x^1$, $q^2 = (0, 0, \dots, 1)^T, \dots, q^{2^d} = (1, \dots, 1)^T \equiv x^1 + \sum_{i=1}^d u^i$. Using this labeling, the k th vertex of the parallelotope can be shown by $x^1 + Uq^k$. Thus, the problem of finding the maximum volume inscribed parallelotope (MVIP) in C can be formulated as the following optimization model:

$$\underset{x^1, \dots, x^{d+1}}{\text{maximize}} \quad \left| \det \begin{pmatrix} x^1 & x^2 & \dots & x^d & x^{d+1} \\ 1 & 1 & \dots & 1 & 1 \end{pmatrix} \right| \quad \text{s.t.} \quad (4.1)$$

$$\begin{aligned} u^i &= x^{i+1} - x^1, & i &= 1, \dots, d \\ x^1 + \sum_{i=1}^d q_i^k u^i &\in C, & k &= 1, \dots, 2^d \end{aligned}$$

where $|\cdot|$ is the absolute value and $\det(\cdot)$ denotes the determinant of a matrix. The objective function calculates the volume of the parallelotope. The first constrain is an auxiliary constraint to define u^i vectors, while the second constraint ensures that all vertices of the parallelotope are inside the convex set C . This is, in general, a non-convex optimization problem with an exponential number of constraints and for general d difficult to solve.

Problem (4.1) can be solved by solving two optimization problems for the positive and negative values of the objective function after removing the absolute value and then choosing the one with the best outcome. The absolute value can also be removed using the epigraph form and rewriting the problem as

$$\begin{aligned} \underset{z, x^1, \dots, x^{d+1}}{\text{maximize}} \quad & z & \text{s.t.} \\ z + (-1)^j \det \begin{pmatrix} x^1 & x^2 & \dots & x^d & x^{d+1} \\ 1 & 1 & \dots & 1 & 1 \end{pmatrix} &\leq 0, & j = 1, 2 \\ u^i &= x^{i+1} - x^1, & i = 1, \dots, d \\ x^1 + \sum_{i=1}^d q_i^k u^i &\in C, & k = 1, \dots, 2^d \end{aligned}$$

However, to keep the model closer to the concept and easier to follow, the mode (4.1) is used for further analysis.

Since we are interested in a parallelotope that is a box (or hypercube), additional orthogonality constraints should be imposed. Hence, the problem of finding MVIR in a convex set $C \in \mathbb{R}^d$ can be formulated as

$$\underset{x^1, \dots, x^{d+1}}{\text{maximize}} \quad \left| \det \begin{pmatrix} x^1 & x^2 & \dots & x^d & x^{d+1} \\ 1 & 1 & \dots & 1 & 1 \end{pmatrix} \right| \quad \text{s.t.} \quad (4.2)$$

$$\begin{aligned} u^i &= x^{i+1} - x^1, & i &= 1, \dots, d \\ (u^i)^T u^j &= 0, & 1 &\leq i < j \leq d \\ x^1 + \sum_{i=1}^d q_i^k u^i &\in C, & k &= 1, \dots, 2^d \end{aligned}$$

In the special case, where the convex set C is a polytope defined by $C = \{x \in \mathbb{R}^d \mid Px \leq b\}$ with $P \in \mathbb{R}^{n \times d}$ and $b \in \mathbb{R}^n$, we have

$$\underset{x^1, \dots, x^{d+1}}{\text{maximize}} \quad \left| \det \begin{pmatrix} x^1 & x^2 & \dots & x^d & x^{d+1} \\ 1 & 1 & \dots & 1 & 1 \end{pmatrix} \right| \quad \text{s.t.} \quad (4.3)$$

$$\begin{aligned} u^i &= x^{i+1} - x^1, & i &= 1, \dots, d \\ (u^i)^T u^j &= 0, & 1 &\leq i < j \leq d \\ v^k &= x^1 + \sum_{i=1}^d q_i^k u^i, & k &= 1, \dots, 2^d \\ Pv^k &\leq b, & k &= 1, \dots, 2^d \end{aligned}$$

where v^k vectors are the vertices of the MVIR.

Both Problems (4.2) and (4.3) are non-convex optimization problems with an exponential number of constraints and difficult to solve.

4.2 MVAIR as an Optimization Problem

In order to find the MVAIR in a compact convex set $C \in \mathbb{R}^d$, additional constraints are needed to impose axis-alignment. In fact, the MVAIR is a box $R = \{x \in \mathbb{R}^d \mid x^l \leq x \leq x^u\}$ of maximum volume inscribed in C , where x^u and x^l are some upper and lower bounds in \mathbb{R}^d , respectively. Hence, it is enough to ensure that for each vertex v^k of R , we have $x^l \leq v^k \leq x^u$, $k = 1, \dots, 2^d$.

Therefore, we obtain

$$\underset{x^1, \dots, x^{d+1}, x^l, x^u}{\text{maximize}} \quad \left| \det \begin{pmatrix} x^1 & x^2 & \dots & x^d & x^{d+1} \\ 1 & 1 & \dots & 1 & 1 \end{pmatrix} \right| \quad \text{s.t.} \quad (4.4)$$

$$\begin{aligned} u^i &= x^{i+1} - x^1, & i &= 1, \dots, d \\ (u^i)^T u^j &= 0, & 1 \leq i < j \leq d \\ v^k &= x^1 + \sum_{i=1}^d q_i^k u^i, & k &= 1, \dots, 2^d \\ v^k &\in C, & k &= 1, \dots, 2^d \\ x^l &\leq v^k \leq x^u, & k &= 1, \dots, 2^d \end{aligned}$$

Note that at optimality, x^l and x^u will coincide with two of the opposing extreme points (vertices) of R . For the special case, where C is a convex polytope, as defined for Problem (4.3), we have

$$\underset{x^1, \dots, x^{d+1}, x^l, x^u}{\text{maximize}} \quad \left| \det \begin{pmatrix} x^1 & x^2 & \dots & x^d & x^{d+1} \\ 1 & 1 & \dots & 1 & 1 \end{pmatrix} \right| \quad \text{s.t.} \quad (4.5)$$

$$\begin{aligned} u^i &= x^{i+1} - x^1, & i &= 1, \dots, d \\ (u^i)^T u^j &= 0, & 1 \leq i < j \leq d \\ v^k &= x^1 + \sum_{i=1}^d q_i^k u^i, & k &= 1, \dots, 2^d \\ P v^k &\leq b, & k &= 1, \dots, 2^d \\ x^l &\leq v^k \leq x^u, & k &= 1, \dots, 2^d \end{aligned}$$

Both Problems (4.4) and (4.5) are also non-convex optimization problems with exponential number of constraints and difficult to solve. However, the structure of the MVAIR problem, i.e., axis-alignment, helps us to improve the efficiency of these models. Consider Problem (4.5). Note that to have $R \subseteq C$, it enforces all of its 2^d vertices to be inside C , hence giving an exponential number of constraints. For this case, we can use a more efficient formulation inspired by a problem in [36]. This new formulation skips the quadratic number, $\mathcal{O}(d^2)$, of the nonlinear perpendicularity constraints $(u^i)^T u^j = 0$ and avoids the exponential number, $\mathcal{O}(n2^d)$, of linear constraints $Pv^k \leq b$. Instead, it deals with $\mathcal{O}(n)$ linear inequality constraints.

Since we have $x_j^l \leq x_j \leq x_j^u$, an upper bound for the left-hand side of each inequality $\sum_j p_{ij} x_j \leq b_i$ is obtained by $\sum_j (p_{ij}^+ x_j^u - p_{ij}^- x_j^l)$, where $p_{ij}^+ = \max\{p_{ij}, 0\}$ and $p_{ij}^- = \max\{-p_{ij}, 0\}$. This means we have $R \subseteq C$ if and only if $\sum_{j=1}^d (p_{ij}^+ x_j^u - p_{ij}^- x_j^l) \leq b_i$, $i = 1, \dots, n$. Hence, we can formulate this problem as:

$$\begin{aligned} \underset{x^l, x^u}{\text{maximize}} \quad & \prod_{j=1}^d (x_j^u - x_j^l) \quad \text{s.t.} \\ & \sum_{j=1}^d (p_{ij}^+ x_j^u - p_{ij}^- x_j^l) \leq b_i, \quad i = 1, \dots, n \\ & x_j^l \leq x_j^u, \quad j = 1, \dots, d \end{aligned}$$

where the objective function calculates the volume of R as the product of the length of d linearly independent vectors corresponding to $d + 1$ affinely independent vertices of R .

Therefore, the problem of finding the MVAIR in a polytope can be efficiently formulated as a convex optimization problem

$$\begin{aligned} \underset{x^l, x^u}{\text{maximize}} \quad & f_0(x^u, x^l) = \sum_{j=1}^d \log(x_j^u - x_j^l) \quad \text{s.t.} \\ & \sum_{j=1}^d (p_{ij}^+ x_j^u - p_{ij}^- x_j^l) \leq b_i, \quad i = 1, \dots, n \end{aligned} \tag{4.6}$$

with the implied constraint $x^u > x^l$, which is easily solvable to the optimality, as described in section 5.1. Note that the number of constraints in this model is exactly the number of

inequalities defining C .

Similarly, the Problem (4.4) can be rewritten in a far more efficient way by incorporating the upper and lower bound points x^u and x^l in the convex inequalities defining C . However, the details of the analysis in this case depends on the definition of C . As an example, consider the convex set $C = \{x \in \mathbb{R}^d \mid x_1 + \dots + x_d \leq 1, x_1^2 + \dots + x_{d-1}^2 - x_d \leq 0\}$, i.e., the intersection of a halfspace and a d -dimensional paraboloid. To have $R \subseteq C$, we must have $v^k \in C$, $k = 1, \dots, 2^d$, which means $v_1^k + \dots + v_d^k \leq 1$ and $\sum_{i=1}^{d-1} (v_i^k)^2 - v_d^k \leq 0$ for $k = 1, \dots, 2^d$. They all can be replaced by only “two” constraints $\sum_{i=1}^d x_i^u \leq 1$ and $\sum_{i=1}^{d-1} (x_i^{\max})^2 - x_d^l \leq 0$, where $x_i^{\max} = \max\{|x_i^l|, |x_i^u|\}$. These two constraints solely depend on the two points x^l and x^u . Using this setting, there is also no need for the remaining constraints in model (4.4). Note that the number of required constraints in this model is also exactly the number of inequalities defining C . The objective function would be the same as that of the Problem (4.6). Therefore, for this convex set, we obtain

$$\begin{aligned}
 & \underset{x^l, x^u}{\text{maximize}} && \sum_{j=1}^d \log(x_j^u - x_j^l) && \text{s.t.} \\
 & && \sum_{i=1}^d x_i^u &\leq 1, \\
 & && \sum_{i=1}^{d-1} (x_i^{\max})^2 - x_d^l &\leq 0, \\
 & && -x_i^{\max} \leq x_i^u \leq x_i^{\max}, & i = 1, \dots, d \\
 & && -x_i^{\max} \leq x_i^l \leq x_i^{\max}, & i = 1, \dots, d
 \end{aligned}$$

which is a convex optimization problem and can be efficiently solved.

Chapter 5

Exact and Approximation Algorithms

In this chapter we present exact and approximation algorithms for finding the maximum volume axis-aligned inscribed rectangle (MVAIR) and the maximum volume inscribed rectangle (MVIR) in a convex set.

5.1 Solving the MVAIR

Here, we introduce an algorithm for finding the MVAIR in a convex polytope and analyze its computational complexity, since the analysis of finding the MVAIR in a general convex set that is defined by a “finite” number of convex inequalities requires to have the specific set of convex inequalities out of various possibilities. However, both the algorithm and the analysis apply to the general convex sets as well.

Having the MVAIR problem modeled as a convex optimization problem enables us to efficiently solve it via efficient convex programming algorithms such as interior-point methods. One of the most efficient interior-point methods for solving convex optimization problems such as MVAIR is the logarithmic barrier method. In addition to the efficiency, the choice of logarithmic barrier method here is also motivated by the fact that the objective function in this method (Eq. (5.2) below) is a closed strictly convex *self-concordant function*

— a class of functions for which the barrier method (with Newton minimization used as a subroutine) provides a rigorous worst-case bound on the number of iterations needed for finding their minimizer, which is useful for the analysis here. Moreover, the convergence analysis is independent of some of the common unknown parameters such as the upper bound on the condition number of the Hessian matrix and its Lipschitz constant, and is also affine invariant, thus insensitive to the choice of coordinates. The latter property is specifically useful for the MVAIR problem as it enables us to rotate or shift the input region in the coordinate system, without changing the worst-case analysis. This worst-case analysis for logarithmic barrier method, which is based on self-concordance properties, was first introduced by Nesterov in [37, 38] and was further developed by Nesterov and Nemirovski in a series of papers including [39, 40, 41] and their seminal book [42]. Note that convex optimization problems can be solved via several efficient algorithms, some of which may provide better practical efficiency. The goal here is not to pinpoint the best algorithm but rather to provide a bound on the computational complexity of solving the MVAIR problem via the convex optimization models described in Section (4.2).

Note that the Problem (4.6) can be rewritten as an unconstrained optimization problem

$$\underset{x^l, x^u}{\text{minimize}} \quad -\sum_{j=1}^d \log(x_j^u - x_j^l) + \sum_{i=1}^n I_{-} \left(\sum_{j=1}^d (p_{ij}^{+} x_j^u - p_{ij}^{-} x_j^l) - b_i \right), \quad (5.1)$$

where the indicator function is defined as

$$I_{-}(y) = \begin{cases} 0 & y \leq 0 \\ \infty & y > 0. \end{cases}$$

In Problem (5.1) the constraints are implicitly incorporated in the objective function.

The indicator barrier function is a non-smooth function. However, we can efficiently approximate it with a logarithmic barrier function, which is smooth. This approximation can be written as $\hat{I}_{-}(y) = -(1/\tau) \log(-y)$ with $\text{dom } \hat{I}_{-} = -\mathbb{R}_{++}$, i.e., the set of strictly negative real numbers. Here $\tau > 0$ is the barrier parameter that controls the accuracy of this approximation. As τ increases in each iteration with $\tau := \mu\tau$, where $\mu > 0$ is an increment parameter, the approximation becomes more accurate. Problem (5.1) can now

be approximated by

$$\underset{x^l, x^u}{\text{minimize}} \quad f(x^u, x^l) = -\tau \left(\sum_{j=1}^d \log(x_j^u - x_j^l) \right) - \left(\sum_{i=1}^n \log \left(b_i - \sum_{j=1}^d (p_{ij}^+ x_j^u - p_{ij}^- x_j^l) \right) \right), \quad (5.2)$$

with $f : \mathbb{R}^{2d} \rightarrow \mathbb{R}$ and the feasible convex and compact domain $G = \{(x^u, x^l) \mid \sum_{j=1}^d (p_{ij}^+ x_j^u - p_{ij}^- x_j^l) - b_i \leq 0, x^l - x^u \leq 0\}$. For simplicity, let x^{ul} to denote the solution pair (x^u, x^l) and let $\phi(x^{ul})$ to denote the barrier term, so we have $f(x^{ul}) = -\tau f_0(x^{ul}) - \phi(x^{ul})$. It is known that by sequentially updating τ with $\tau := \mu\tau$ we converge to the optimal solution when $\tau \rightarrow \infty$ tracing a central path $\mathcal{P} = \{x^{ul*}(\tau) : \tau \geq 0\}$ [42, 43]. The objective function f is closed, smooth, continuously differentiable, and strictly convex. In addition, f is a self-concordant function for G for all real values of $\tau \geq 0$. This is due to the invariance property of self-concordant functions under scaling and addition operations and the fact that each of the negative logarithm terms is a self-concordant function.

Let's begin the analysis with the pre-processing operations. The first observation is that we can fairly assume that the Problem (4.6) is strictly feasible as C is a compact convex set with a non-empty interior. This means the Slater's condition holds. To find a strictly feasible solution as the starting point of the algorithm, which removes the necessity of an infeasible start step and simplifies the analysis, choose $d + 1$ arbitrary but affinely independent points on the boundary of C . For a polytope this is readily available by the given set of vertices of C . For a general convex set C , this would depend on the structure of C . Given the $d + 1$ points $p^1, \dots, p^{d+1} \in \partial C$, the simplex $S = \mathbf{Conv}(p^1, \dots, p^{d+1}) \subset C$. Let $h_1 = \mathbf{Conv}(p^1, p^2, \dots, p^d)$ and $h_2 = \mathbf{Conv}(p^1, p^3, \dots, p^{d+1})$ be two of the facets of S . Let y^1 and y^2 be the median points of h_1 and h_2 , respectively. Each of these median points could be found by solving a d -dimensional Fermat (1-median) problem with d input points. We shall have $y^1 \neq y^2$ since the points p^1, \dots, p^{d+1} were affinely independent. Let the pair

$$x_{init}^u = \begin{pmatrix} \max\{y_1^1, y_1^2\} \\ \max\{y_2^1, y_2^2\} \\ \vdots \\ \max\{y_d^1, y_d^2\} \end{pmatrix}, \quad x_{init}^l = \begin{pmatrix} \min\{y_1^1, y_1^2\} \\ \min\{y_2^1, y_2^2\} \\ \vdots \\ \min\{y_d^1, y_d^2\} \end{pmatrix},$$

be the initial strictly feasible solution. Note that $x_{init}^{ul} = (x_{init}^u, x_{init}^l)$ could be a degenerate solution, i.e., we could have $\mathbf{Vol}(R_{init}) = 0$.

An alternative way for constructing x_{init}^{ul} that works for all convex sets is as follows. Find B the minimum volume axis-aligned bounding box of the convex domain $G = \{(x^u, x^l) \mid x^l \in C, x^u \in C, x^l - x^u \leq 0\}$ and then let y^1 and y^2 be the diagonally opposing vertices of B with the minimum and the maximum coordinates, respectively. Set $x_{mid}^{ul} = 1/2(y^1 + y^2)$. We have $x_{mid}^{ul} \in G$, since $\mathbf{Vol}(G) \geq \mathbf{Vol}(B)/2$ due to the convexity of G . If $x_{mid}^{ul} \in \mathbf{int} G$ then set $x_{init}^{ul} := x_{mid}^{ul}$. Otherwise, find the vector $\nu = e^k - \frac{(e^k)^T(y^2 - y^1)}{\|y^2 - y^1\|^2}(y^2 - y^1)$, where index k corresponds to the smallest component of $(y^2 - y^1)$ and e^k is the k th column of the $d \times d$ identity matrix. Then, find a sufficiently small $\delta_1 > 0$ such that either $x_{mid}^{ul} + \delta_1 \nu$ or $x_{mid}^{ul} - \delta_1 \nu$ is in the interior of G , i.e., strictly feasible. To increase the depth of strict feasibility of the initial solution and thus its quality we can take one further step. Without loss of generality, assume the direction $-\nu$ gives the strictly feasible solution. Let δ_2^{max} be the maximum value of $\delta_2 > \delta_1$ such that $x_{mid}^{ul} - \delta_2 \nu \in G$. Let $x_{ray}^{ul} = x_{mid}^{ul} - \delta_2^{max} \nu$ and set $x_{init}^{ul} := 1/2(x_{mid}^{ul} + x_{ray}^{ul})$.

The logarithmic barrier method, described in Algorithm 1, has an outer iteration loop in which the barrier parameter is updated and an inner iteration loop (centering step) in which usually Newton's method, with a backtracking line search for finding a reasonable step size in each iteration, is used to reach the minimizer for any given τ . Based on the analysis of log-barrier method for self-concordant convex functions, the logarithmic barrier method spends $N^{(0)}$ iterations (Newton steps) in the first centering step to reach a point sufficiently close to the central path of Problem (5.2). It then takes $N^{(CP)}$ iterations (Newton steps) in the path following step, during which the algorithm iteratively updates the parameter τ with $\tau := \mu\tau$ and tries to follow the central path as $\tau \rightarrow \infty$, to get sufficiently close to the optimal solution. Note that the other end of this central path that is associated with $\tau \rightarrow +0$ is the analytic center of the G with respect to the barrier function ϕ . Therefore, the total number of iterations required to solve Problem (5.2) using the logarithmic barrier method is $N = N^{(0)} + N^{(CP)}$.

For the number of iterations in the initial centering step, we need to define the Minkowsky

Input: Given $\tau := \tau^{(0)} > 0$, $\mu > 1$, tolerance $\varepsilon > 0$, and a strictly feasible solution x_0^{ul} within proximity $\kappa > 0$ of \mathcal{P} .

Output: An ε -approximation solution to the optimal solution.

while $m/t \geq \varepsilon$ **do**

 /* Centering Step

*/

 Compute $x^{ul*}(\tau)$ by minimizing $f(x^{ul}) = -\tau f_0(x^{ul}) - \phi(x^{ul})$, starting at $x^{ul}(\tau)$;

 /* Path Following Step

*/

 Set $x^{ul}(\tau) := x^{ul*}(\tau)$;

 Set $\tau := \mu\tau$;

end

return $x^{ul*}(\tau)$ and $f_0(x^{ul*}(\tau))$;

Algorithm 1: LogarithmicBarrierAlgorithm; it solves a constrained convex optimization problem with sequence of unconstrained optimization problems, where the obtained minimizer of each iteration is used as the starting point of the next iteration.

function of a convex domain.

Definition 13. The Minkowsky function of a convex domain G with the pole at $x \in G$ is

$$\pi_x(y) = \inf\{\eta \geq 0 \mid x + \eta^{-1}(y - x) \in G\}$$

Geometrically speaking, consider a ray $[x, y)$ and let y' be the point this ray intersect ∂G . If y' exists, then $\pi_x(y)$ is the length of the segment $[x, y]$ divided by the length of the segment $[x, y']$. If G is unbounded and the ray $[x, y)$ is contained in G , then $\pi_x(y) = 0$. In other words, $\pi_x(y)$ measures the distance between x and y relative to the distance of x to the boundary of G in the direction $y - x$.

For the main path following scheme to work, we need to start from an initial point sufficiently close to the central path \mathcal{P} . We can first move from $x_{init}^{ul} \in \text{int } G$ to the beginning of the central path, i.e., the analytic center $x_{ac}^{ul} \in \mathcal{P}$, and from there, we can follow \mathcal{P} to converge to the optimal solution. It is proven that, with tolerance κ , we can

converge to the analytic center x_{ac}^{ul} starting from the strictly feasible solution x_{init}^{ul} in

$$N^{(0)} = \mathcal{O}(1) \sqrt{n} \log \left(\frac{n}{1 - \pi_{x_{ac}^{ul}}(x_{init}^{ul})} \right),$$

Newton iterations, where $\mathcal{O}(1)$ are constant factors depending solely on the path tolerance κ and the penalty rate used in this initial centering step [44]. The tolerance (accuracy) in this step does not need to be very small. Also, note that $0 \leq \pi_{x_{ac}^{ul}}(x_{init}^{ul}) < 1$, since $x_{init}^{ul} \in \text{int } G$. The smaller it is the better our initial solution x_{init}^{ul} , i.e., further away from the boundary and closer to the analytic center. Due to the construction of x_{init}^{ul} , we expect the ratio $\frac{1}{1 - \pi_{x_{ac}^{ul}}(x_{init}^{ul})} > 1$ to be fairly small for all instances of the problem. Since it still depends on the unknown point x_{ac}^{ul} , we can bound with a *symmetry measure* proposed by Minkowski [45].

Definition 14. The Minkowski symmetry measure of a convex set G with respect to $x \in G$ is defined as

$$\text{sym}_G(x) = \max\{\eta \geq 0 : x + \eta(x - y) \in G, \forall y \in G\}$$

Note that $\text{sym}_G(x) = 0$, when $x \in \partial G$, and $\text{sym}_G(x) \leq 1$, where the equality holds when G is symmetric around x , which also means G is symmetric.

Let $x' = x_{ac}^{ul} + \frac{1}{\pi_{x_{ac}^{ul}}(x_{init}^{ul})}(x_{init}^{ul} - x_{ac}^{ul})$ be the point on the boundary of G where the ray $[x_{ac}^{ul}, x_{init}^{ul})$ crosses the boundary. We have

$$\begin{aligned} 1 - \pi_{x_{ac}^{ul}}(x_{init}^{ul}) &= 1 - \frac{\text{dist}(x_{init}^{ul}, x_{ac}^{ul})}{\text{dist}(x', x_{ac}^{ul})} = \frac{\text{dist}(x', x_{init}^{ul})}{\text{dist}(x', x_{ac}^{ul})} \\ &= \max\{\tau \geq 0 : x_{init}^{ul} + \tau(x_{init}^{ul} - x_{ac}^{ul}) \in G\} \geq \text{sym}_G(x_{init}^{ul}) > 0 \end{aligned}$$

Therefore, we have

$$N^{(0)} = \mathcal{O}(1) \sqrt{n} \log \left(\frac{n}{1 - \pi_{x_{ac}^{ul}}(x_{init}^{ul})} \right) \leq \mathcal{O}(1) \sqrt{n} \log \left(\frac{n}{\text{sym}_G(x_{init}^{ul})} \right),$$

Note that the algorithm does not need to compute $\text{sym}_G(x_{init}^{ul})$.

To start the main path following scheme, in Algorithm 1, we can let x_0^{ul} to be the

approximate solution $\widehat{x_{ac}^{ul}}$ achieved in the initialization phase for x_{ac}^{ul} and set

$$\tau^{(0)} = \max\{\tau \mid \lambda(\widehat{x_{ac}^{ul}}) \leq \kappa\}, \quad (5.3)$$

where $\tau^{(0)}$ is the initial choice of barrier parameter for the main path following step and $\lambda(x)$ is the Newton decrement defined as $\lambda(x) = \sqrt{\nabla f(x) \nabla^2 f(x)^{-1} \nabla f(x)}$ with f being the objective function in (5.2). For the number of iterations during the main path following phase, we have

$$\begin{aligned} N^{(CP)} &= \left\lceil \frac{\log\left(\frac{n}{\tau^{(0)}\varepsilon}\right)}{\log \mu} \right\rceil \left(\frac{f(x^{ul*}(\tau)) - f(x^{ul*}(\mu\tau))}{\gamma} + \log_2 \log_2\left(\frac{1}{\varepsilon}\right) \right) \\ &= \left\lceil \frac{\log\left(\frac{n}{\tau^{(0)}\varepsilon}\right)}{\log \mu} \right\rceil \left(\frac{n(\mu - 1 - \log \mu)}{\gamma} + c \right) \\ &= \left\lceil \sqrt{n} \log_2\left(\frac{n}{\tau^{(0)}\varepsilon}\right) \right\rceil \left(\frac{1}{2\gamma} + c \right) \\ &\leq \left(1 + \sqrt{n} \log_2\left(\frac{n}{\tau^{(0)}\varepsilon}\right) \right) \left(\frac{1}{2\gamma} + c \right), \end{aligned}$$

where n is the number of inequalities defining the polytope, γ is a constant lower bound (given in Eq. (5.4) below) on the reduction amount in the objective function in each iteration during the damped Newton phase, ε is the required accuracy for the optimal solution, $c = \log_2 \log_2(1/\varepsilon)$, and the pair $(x^{ul*}(\mu\tau))$ is the optimal solution of the centering step starting from $(x^{ul*}(\tau))$ after updating the barrier parameter in the outer loop. In the first equality, the first term is the number of iterations in the outer loop and the second term is the number of Newton steps in the inner loop per centering iteration. The ratio $n/\tau^{(0)}$ is the initial duality gap and ε is, in fact, the final duality gap. The second equality is derived by extracting the dual function in the first fraction of the second term and then simplifying it using the duality gap when the barrier parameter is τ . The third equality is derived by assuming a fixed value for μ as $\mu = 1 + 1/\sqrt{n}$.

The term $c = \log_2 \log_2(1/\varepsilon)$ is an upper bound on the number of iterations during the quadratically convergent phase of Newton's method and has a very weak dependence on the inverse of ε and can be effectively considered as constant; for $\varepsilon = 10^{-9}$, this is less than

5. Also, the parameter γ depends, weakly, on the backtracking line search parameters α and β and is equal to

$$\gamma = \frac{\alpha\beta(1-2\alpha)^2}{20-8\alpha}, \quad (5.4)$$

where $0 < \alpha < 0.5$ and $0 < \beta < 1$. For $\alpha = 0.2$ and $\beta = 0.9$, we have $\frac{1}{2\gamma} < 142$. Finally, note that $N^{(CP)}$ does not depend on the dimension d .

Finally, the total number of Newton steps is

$$N = N^{(0)} + N^{(CP)} \leq \mathcal{O}(1) \sqrt{n} \log_2 \left(\frac{n}{(\text{sym}_G(x_{init}^{ul}))\tau^{(0)}\varepsilon} \right),$$

where $\mathcal{O}(1)$ is an absolute constant. Following a more refined analysis, such as the original analysis of Nesterov and Nemirovski [42], the bound could be tightened by finding smaller and more accurate constants. Furthermore, by carefully choosing the input parameters of the method the condition in Eq. (5.3) can be guaranteed and $\tau^{(0)}$ can be removed from the right hand side of the bound. Hence, the process is terminated with an ε -solution in $N = \mathcal{O}(\sqrt{n} \log(\frac{n}{\varepsilon}))$ iterations. Alternatively, if we can establish a strictly feasible dual solution, then the ratio $n/\tau^{(0)}$ can be replaced by the constant ε_0 , the initial duality gap, leading to $\mathcal{O}(\sqrt{n} \log(\frac{\varepsilon_0}{\varepsilon}))$ run time. Note that this is a conservative upper bound and in practice the algorithm performs better, in many cases just in a few iterations independent of the size of the problem. In general, the observed average run time of path following methods is $\mathcal{O}(\log n \log(\frac{\varepsilon_0}{\varepsilon}))$ [46].

Each Newton step (inner iteration) is equivalent with solving a linear system of equations $H\Delta x^{ul} = -g$, where $H = \nabla^2 f(x^{ul})$ is the Hessian matrix, $g = \nabla f(x^{ul})$ is the gradient vector, and Δx^{ul} is the Newton direction. This will cost $\mathcal{O}((2d)^3)$ arithmetic operations for solving the linear system plus the costs of computing (forming) g and H . Computing g and H require at most $(2d \times (n+1)) = \mathcal{O}(dn)$ and $((2d)^2 \times (n+1)) = \mathcal{O}(d^2n)$ operations, respectively. Therefore, the computational complexity of the log-barrier method for solving Problem (4.6) in each step is $\mathcal{O}(d^3 + d^2n)$. Nevertheless, certain structures of the problem could be exploited to reduce this bound in practice.

Therefore, the total computational complexity of solving Problem (4.6) using the log-barrier method is $\mathcal{O}((d^3 + d^2n)\sqrt{n} \log \frac{n}{\varepsilon})$. For a polytope, since C is bounded we have $n > d$ and thus d^3 is dominated by d^2n leading to $\mathcal{O}(d^2n\sqrt{n} \log \frac{n}{\varepsilon})$ time.

Since this analysis is not based on an assumption restricting it to polytopes, the result is the same for finding the MVAIR in general convex sets, such as d -ellipsoids, which can be easily represented in a finite set of inequalities. For example, for d -dimensional ellipses we obtain $\mathcal{O}(d^3)$ running time since we just need one inequality to define an ellipsoidal convex set.

Finally, it should be mentioned that since the Fermat problem could be formulated as a second-order cone program (SOCP), the preprocessing time for finding the initial strictly feasible solution takes at most $\mathcal{O}(d^3\sqrt{d} \log \frac{1}{\varepsilon_f})$ time using the primal-dual potential reduction algorithm of [47]. Here, ε_f is the accuracy for finding the exact Fermat point, which could be considered a fairly large number (e.g., 10^{-1}) as the exact Fermat point is not needed for constructing R_{init} . So the pre-processing time the first way of finding x_{init}^{ul} is essentially $\mathcal{O}(d^3\sqrt{d})$. The pre-processing time for the alternative way depends on the geometry of C and the algorithm used for finding its minimum volume axis-aligned bounding box. Let $T_x(C)$ be the time that it takes to find an extreme point in a given direction in a convex set C . Then this box can be found in $\mathcal{O}(dT_x(C))$. For a convex polygon, this can be done in $\mathcal{O}(\log n)$ using binary search, if the n vertices are given as an array in a c.w. or c.c.w. order. It must be mentioned that this preprocessing for finding a strictly feasible starting point is not an essential part of the algorithm as the algorithm could have an infeasible starting point for the initial centering step. However, in that case, the analysis and the upper bound on the number of iterations N are a bit different, although the bound would still grow with $\sqrt{n} \log \frac{n}{\varepsilon}$.

The following theorem summarizes the complexity analysis of solving MVAIR.

Theorem 15. *The problem of finding the MVAIR in a convex set in \mathbb{R}^d defined by n convex inequalities can be solved to an ε -approximation by the logarithmic barrier algorithm in $\mathcal{O}((d^3 + d^2n)\sqrt{n} \log \frac{n}{\varepsilon})$ time.*

Remark 1. It is worth noting that the ε -approximation solution can be rounded to the optimal solution in a precise way. Having an ε -approximation solution with $\varepsilon \leq 2^{-2L}$, where L is the size of the problem defined as the binary input length of the problem, i.e., the number of bits needed to encode the problem, the optimal solution can be achieved in a rounding procedure with a polynomial number of elementary operations (in terms of the dimension d) as suggested in [48, 49].

5.2 Solving the MVIR

As discussed in Section 4.1, the MVIR problem in the higher dimension, i.e., the Problem (4.2), is a non-convex optimization problem with an exponential number of constraints and is difficult to solve even for the special case of Problem (4.3), where the convex set C is a polytope. Solving the MVIR problem efficiently in higher dimensions would require further exploitation of the structure of the problem and the properties of the optimal solution that is considered as a future research direction for this study. In the rest of this section, we limit ourselves to the 2D version, which is the MAIR problem.

A Parametric Approach for Finding the MAIR

This section provides a parametrized optimization approach for the MAIR problem in a compact convex set $C \subset \mathbb{R}^2$. Consider the 2D version of the Problem (4.2) and let $u = u^1$, $v = u^2$, $x = x^1$, $y = x^2$, $z = x^3$; see Figure 1.1 for an illustration for the special case when C is a convex polygon. Then finding the MAIR in C can be formulated as:

$$\begin{aligned}
 (Q) \quad & \text{maximize} \quad |\det(u, v)| \\
 & \text{s.t.} \quad u^T v = 0 \\
 & \quad u = y - x, v = z - x \\
 & \quad x, y, z, y + z - x \in C \subset \mathbb{R}^2.
 \end{aligned}$$

Clearly, the last two constraints in (Q) can be rewritten as $(u, v) \in S \subseteq \mathbb{R}^4$, where $S = \{(u, v) \mid u = y - x, v = z - x, \text{ and } x, y, z, y + z - x \in C\}$ is a compact convex set. We

have

$$(Q') \quad \begin{array}{ll} \text{maximize} & |u_1 v_2 - u_2 v_1| \\ \text{s.t.} & u_1 v_1 + u_2 v_2 = 0 \\ & (u, v) \in S \subset \mathbb{R}^4. \end{array}$$

Introducing a parameter $u_2/u_1 = t$ and $v_2/v_1 = -1/t$, the above problem reduces to a parameterized model

$$(Q_t) \quad \begin{array}{ll} \text{maximize} & (1 + t^2)|u_1 v_2| \\ \text{s.t.} & u_2 - t u_1 = 0, v_1 + t v_2 = 0, \\ & (u, v) \in S \subset \mathbb{R}^4. \end{array}$$

For any fixed t , (Q_t) can be solved by sequentially solving four separate subproblems:

$$\begin{array}{ll} \text{maximize} & u_1 v_2 \\ \text{s.t.} & u_1 \geq 0, v_2 \geq 0, \\ & u_2 - t u_1 = 0, v_1 + t v_2 = 0, \\ & (u, v) \in S \subset \mathbb{R}^4; \end{array}$$

$$\begin{array}{ll} \text{maximize} & u_1 v_2 \\ \text{s.t.} & u_1 \leq 0, v_2 \leq 0, \\ & u_2 - t u_1 = 0, v_1 + t v_2 = 0, \\ & (u, v) \in S \subset \mathbb{R}^4; \end{array}$$

$$\begin{array}{ll} \text{maximize} & -u_1 v_2 \\ \text{s.t.} & u_1 \geq 0, v_2 \leq 0, \\ & u_2 - t u_1 = 0, v_1 + t v_2 = 0, \\ & (u, v) \in S \subset \mathbb{R}^4; \end{array}$$

$$\begin{array}{ll} \text{maximize} & -u_1 v_2 \\ \text{s.t.} & u_1 \leq 0, v_2 \geq 0, \\ & u_2 - t u_1 = 0, v_1 + t v_2 = 0, \\ & (u, v) \in S \subset \mathbb{R}^4. \end{array}$$

Clearly these four models are easily solvable; we may invoke any convex optimization solver to solve their respective equivalent convex optimization forms:

$$\begin{array}{ll} \text{maximize} & \log u_1 + \log v_2 \\ \text{s.t.} & u_2 - t u_1 = 0, v_1 + t v_2 = 0, \\ & (u, v) \in S \subset \mathbb{R}^4; \end{array}$$

$$\begin{array}{ll} \text{maximize} & \log(-u_1) + \log(-v_2) \\ \text{s.t.} & u_2 - t u_1 = 0, v_1 + t v_2 = 0, \\ & (u, v) \in S \subset \mathbb{R}^4; \end{array}$$

$$\begin{aligned}
& \text{maximize} && \log u_1 + \log(-v_2) \\
& \text{s.t.} && u_2 - tu_1 = 0, v_1 + tv_2 = 0, \\
& && (u, v) \in S \subset \mathbb{R}^4;
\end{aligned}$$

$$\begin{aligned}
& \text{maximize} && \log(-u_1) + \log v_2 \\
& \text{s.t.} && u_2 - tu_1 = 0, v_1 + tv_2 = 0, \\
& && (u, v) \in S \subset \mathbb{R}^4.
\end{aligned}$$

Let the optimal value of (Q_t) be $f(t)$. Finding the maximum area rectangle inside S can be achieved by sequentially solving the parameterized problems and then identifying t to maximize $f(t)$.

Observe that x, y, z are chosen arbitrarily in C , and the role of $u = y - x$ and $v = z - x$ are symmetric. Therefore, one does not need to go through all four cases; it suffices to focus only on the first case, and the parameter t can also be restricted to be nonnegative. In other words, we need only to consider

$$\begin{aligned}
& \text{maximize} && \log u_1 + \log v_2 \\
& \text{s.t.} && u_2 - tu_1 = 0, v_1 + tv_2 = 0, \\
& && (u, v) \in S \subset \mathbb{R}^4,
\end{aligned} \tag{5.5}$$

for any given nonnegative t . This is a convex optimization problem, for any fixed t , that has a *unique* optimal solution (i.e., the MAIR with respect to the direction t), since the feasibility set is nonempty, compact, and convex, and the objective function is closed and strictly concave. Let $\psi(t)$ to denote the optimal value function of (5.5). Then, $f(t) = (1 + t^2)e^{\psi(t)}$, and the parametric search in (Q_t) boils down to the one-dimensional optimization: $\text{maximize}_{t \geq 0} f(t)$.

To make the domain of t bounded, we need one more step. By definition of t , we have $t = \tan(\theta)$, where θ is the angle between the x -axis and vector u . Then, $t \geq 0$ is equivalent to $\theta \in [0, \pi/2]$.

Observation 16. Any rectangle with $\pi/4 < \theta < \pi/2$ has an identical counterpart with $\theta \in (-\pi/4, 0)$, which satisfies conditions $u(1) > 0$, $v(2) > 0$ and can be obtained by the linear transformation $z \rightarrow x'$, $x \rightarrow y'$, $y + z - x \rightarrow z'$, $u' = -v$, $v' = u$. Between the

identical rectangles, we have $|\theta - \theta'| = \pi/2$. Using the same transformation, we obtain that the rectangle with $\theta = \pi/2$ is identical to the rectangle with $\theta' = 0$ and also the rectangles with $\theta = \pi/4$ and $\theta' = -\pi/4$ are identical. Therefore, it suffices to consider only the rectangles with $\theta \in [-\pi/4, \pi/4]$, or equivalently $t \in [-1, 1]$.

Thus, the problem of finding the MAIR in a convex set $C \subset \mathbb{R}^2$ is

$$\begin{aligned} \underset{t}{\text{maximize}} \quad & f(t) = (1 + t^2)e^{\psi(t)} \quad \text{s.t.} \\ & -1 \leq t \leq 1, \end{aligned} \tag{5.6}$$

where $\psi(t)$ is the optimal value of (5.5). This problem has an optimal solution by the following proposition.

Proposition 17. *The function $f(t)$ attains its maximum.*

Proof. Since (5.5) is a convex optimization problem for any given t , its set of maximizers is also convex. Moreover, the feasibility set of (5.5) is compact, its objective function is closed, and Slater's condition holds. Therefore, the set of maximizers is nonempty, closed, and bounded as well; in fact, it is a singleton due to the strict concavity of the objective function. Adding the fact that the linear independence constraint qualification (LICQ) holds for the optimal solution $(u^*(\bar{t}), v^*(\bar{t}))$ for any given \bar{t} , we obtain that the optimal value function $\psi(t)$ is upper semi-continuous on its domain $-1 \leq t \leq 1$ [50, 51]. Hence, the function $f(t)$ is upper semi-continuous on $-1 \leq t \leq 1$, since e^x is continuous on \mathbb{R} and the function $(1 + t^2)$ is continuous on $-1 \leq t \leq 1$. Moreover, the domain of t is a compact set, i.e., the interval $[-1, 1]$. Therefore, by the Weierstrass extreme value theorem, $f(t)$ attains its supremum. \square

However, finding this maximum could be difficult. This is because the function $f(t)$ is not explicitly formulated, since it depends on $\psi(t)$, and it has some undesirable properties. Although it is an upper semi-continuous and univariate function, it is also non-smooth, non-differentiable, non-unimodal, and non-concave and in some cases, it could be a very ill-behaved function (see Figures 6.1a and 6.2c). Therefore, it is very difficult to design an

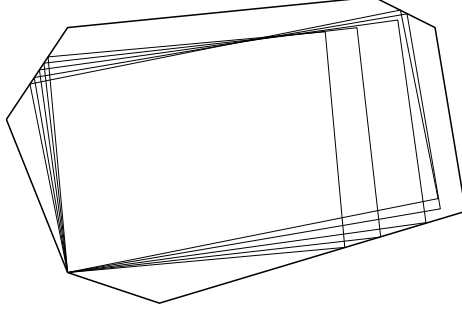


Figure 5.1: Sensitivity of the inscribed rectangles to the direction assuming a fixed vertex-corner.

algorithm that guarantees to find the optimal solution. Figure 5.1 visualizes this difficulty by showing the sensitivity of the area of the inscribed rectangles to the direction t . Nevertheless, being restricted to a one-dimensional search enables us to develop a good approximation algorithm.

Such an algorithm will not only solve the MAIR problem but also provides, by fixing the direction, a much more general algorithm for the 2-dimensional case of the MVAIR, i.e., the MAAIR problem in a convex set $C \subset \mathbb{R}^2$. It is a more general algorithm than the interior point algorithm presented in Section 5.1, in the sense that it finds the largest rectangle aligned to not only the regular axes but also to any rotated axes in any direction.

An Exact Algorithm for Finding the MAAIR in any Given Direction

We provide an optimization approach for finding the largest inscribed rectangle in any given direction, i.e. aligned to any rotated axes, in a convex set. The following theorem states the main result of this section.

Theorem 18. *For a compact convex set, $C \subset \mathbb{R}^2$ defined by n convex inequalities, the MAAIR regarding the perpendicular axes in any given direction can be found in $\mathcal{O}(n\sqrt{n}(\log n + 2L))$ time.*

Proof. Let's assume, without loss of generality, that C is a convex polygon. The problem

(5.5) can be expanded as

$$\text{maximize } \log u_1 + \log v_2 \quad (5.7)$$

s.t.

$$\begin{aligned} u_2 - tu_1 &= 0 \\ v_1 + tv_2 &= 0 \\ u - y + x &= 0 \\ v - z + x &= 0 \\ Px &\leq b \\ Py &\leq b \\ Pz &\leq b \\ P(y + z - x) &\leq b \end{aligned}$$

where $P \in \mathbb{R}^{n \times 2}$ and $b \in \mathbb{R}^n$ are the given characterizations of the convex polygon C . Putting $t = 0$ gives the MAAIR with respect to the regular (non-rotated) axes. The assumption of C being a polygon is not restrictive since problem (5.7) can be defined similarly for any other closed and bounded convex set that can be defined with a “finite” number of convex inequalities.

Suppose t is given. We can rewrite (5.7) in the matrix form. Define $s = (u^T v^T x^T y^T z^T)^T$, which is a 10×1 vector. Then we have

$$\text{minimize } -(\log e_1^T s + \log e_4^T s) \quad (5.8)$$

s.t.

$$\begin{aligned} As &= 0 \\ \tilde{P}s &\leq \tilde{b} \end{aligned}$$

where e_i is the i th column of a 10-by-10 identity matrix, $\tilde{b} = (b_1, b_1, b_1, b_1, b_2, b_2, b_2, b_2, \dots, b_n, b_n, b_n, b_n)^T$, i.e. a $4n \times 1$ vector, and A is

$$A = \begin{bmatrix} -t & 1 & 0 & 0 & 0 & 0 & 0 & 0 & 0 & 0 \\ 0 & 0 & 1 & t & 0 & 0 & 0 & 0 & 0 & 0 \\ 1 & 0 & 0 & 0 & 1 & 0 & -1 & 0 & 0 & 0 \\ 0 & 1 & 0 & 0 & 0 & 1 & 0 & -1 & 0 & 0 \\ 0 & 0 & 1 & 0 & 1 & 0 & 0 & 0 & -1 & 0 \\ 0 & 0 & 0 & 1 & 0 & 1 & 0 & 0 & 0 & -1 \end{bmatrix}_{(6 \times 10)}$$

and \tilde{P} is

$$\tilde{P} = \begin{bmatrix} 0 & 0 & 0 & 0 & p_{11} & p_{12} & 0 & 0 & 0 & 0 \\ 0 & 0 & 0 & 0 & 0 & 0 & p_{11} & p_{12} & 0 & 0 \\ 0 & 0 & 0 & 0 & 0 & 0 & 0 & 0 & p_{11} & p_{12} \\ 0 & 0 & 0 & 0 & -p_{11} & -p_{12} & p_{11} & p_{12} & p_{11} & p_{12} \\ \cdots & & & & \cdots & & & & & \\ \vdots & & & & \ddots & & & & & \\ 0 & 0 & 0 & 0 & p_{n1} & p_{n2} & 0 & 0 & 0 & 0 \\ 0 & 0 & 0 & 0 & 0 & 0 & p_{n1} & p_{n2} & 0 & 0 \\ 0 & 0 & 0 & 0 & 0 & 0 & 0 & 0 & p_{n1} & p_{n2} \\ 0 & 0 & 0 & 0 & -p_{n1} & -p_{n2} & p_{n1} & p_{n2} & p_{n1} & p_{n2} \end{bmatrix}_{(4n \times 10)}$$

The log-barrier function is

$$f(s) = -\tau \left(\log e_1^T s + \log e_4^T s \right) - \left(\sum_{i=1}^6 \log(-a_i^T s) + \sum_{i=1}^6 \log(a_i^T s) \right) - \left(\sum_{i=1}^{4n} \log(\tilde{b}_i - \tilde{p}_i^T s) \right)$$

The above function is $f : \mathbb{R}^{10} \rightarrow \mathbb{R}$ and convex, hence this is a convex optimization problem with constant size in dimension. Therefore, by Theorem 15, for any fixed direction $-1 \leq t \leq 1$, including the traditional axis-aligned case ($t = 0$), this can be solved to optimality by the logarithmic barrier algorithm in $\mathcal{O}(n\sqrt{n}(\log n + 2L))$ time. \square

Remark 2. This result is more general than the existing results such as the algorithm of Alt et al. [30], as it deals with general convex sets, compared to the existing results that are limited to convex polygons. Moreover, it can find the MAAIR aligned to any rotated axes. For a convex polygon with n vertices, one could find the rotated coordinates of all vertices in linear time and then perform one of the existing axis-aligned algorithms. However, for general sets, such change of coordinates could be computationally very expensive, and yet after such rotation, one would need an algorithm capable of finding MAAIR in general convex sets.

Remark 3. It is important to observe that this computational complexity depends only on n , the number of convex inequalities defining the set C . For example, for ellipses, it will be $\mathcal{O}(1)$ since only one inequality defines an ellipsoidal convex set.

An Approximation Algorithm for Finding the MAIR

We can use this fast exact algorithm, that finds the largest rectangle in any given direction inscribed in a compact convex set $C \subset \mathbb{R}^2$, as a subroutine to obtain an approximation algorithm for the case where we want to find the largest inscribed rectangle among all directions, i.e., the MAIR.

Consider a compact and convex set $C \in \mathbb{R}^2$. We seek to solve the Problem (5.6), which has a univariate objective function $f(t) = (1 + t^2)e^{\psi(t)}$, where $\psi(t)$ is the optimal value of (5.5). For simplicity, in this section, we use the notation $|\cdot|$ as a measure of both area and length. Let R_{opt} to be the optimal solution and R_{apx} to be the ε -approximation solution, i.e. $|R_{apx}| \geq (1 - \varepsilon)|R_{opt}|$. The basic intuition is that the direction of an ε -approximation solution should be very close to the direction of the optimal rectangle. Suppose the optimal rectangle happens at direction angle θ^* . We want to know how much the area of the rectangle changes if we change the direction slightly. So we want to find a lower bound for the area of an approximation rectangle with direction angle $\theta_{apx} \in [\theta^* - \alpha, \theta^* + \alpha]$, for some small $\alpha > 0$.

Lemma 19. *Let $C \subset \mathbb{R}^2$ be a compact convex set and $R_{opt} \subset C$ be the MAIR. The aspect ratio $\rho = \text{AR}(R_{opt})$ is bounded from above. When C is a polygon an upper bound that only depends on C can be obtained in linear time and an upper bound that depends on an outer approximation of C can be obtained in logarithmic time.*

Proof. Let $w \geq h > 0$ be the side lengths of R_{opt} . Also, let R_{diam} be the minimum area rectangle enclosing C such that its longer side is parallel to a $\text{diam}(C)$ with the same length. Let $h_{diam} \leq \text{diam}(C)$ be the length of the side of R_{diam} that is perpendicular to $\text{diam}(C)$, i.e., the width of C when seen from the same direction angle of $\text{diam}(C)$. See Figure 5.2 for an illustration. By the fact that $C \subset R_{diam}$ and the convexity of C we have

$$\frac{\text{diam}(C)h_{diam}}{2} = \frac{|R_{diam}|}{2} \leq |C| \leq |R_{diam}| = \text{diam}(C)h_{diam}$$

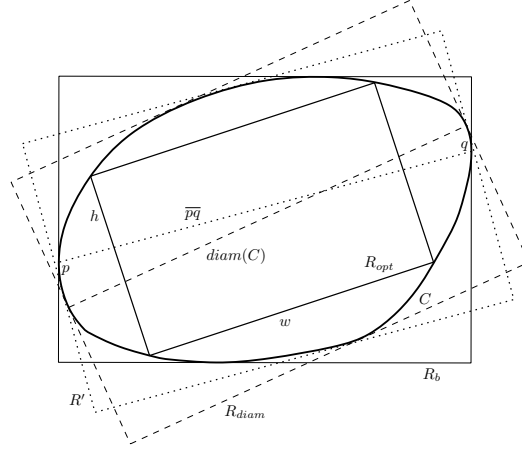


Figure 5.2: An illustration of the proof of Lemma 19 for the upper bound on the aspect ratio of the MAIR in a convex set. The dashed rectangle is induced by the diameter of the set and the dotted rectangle is induced by the line segment that connects the touching points of the set and the shorter sides of its smallest axis-aligned bounding box.

Using Lassak's bound [23], we have $wh = |R_{opt}| \geq |C|/2$. Therefore,

$$\text{diam}(C)h \geq wh = |R_{opt}| \geq |C|/2 \geq \frac{|R_{diam}|}{4} = \frac{\text{diam}(C)h_{diam}}{4} \geq \frac{|C|}{4},$$

which gives $h \geq h_{diam}/4 \geq \frac{|C|}{4 \text{diam}(C)}$. Hence

$$\rho = \text{AR}(R_{opt}) = \frac{w}{h} = \frac{\text{diam}(C)}{h_{diam}/4} \leq \frac{4(\text{diam}(C))^2}{|C|} = 4 \text{AR}_{cvx}(C) \quad (5.9)$$

If the geometry of C is such that $|C|$ and $\text{diam}(C)$ can be computed in constant time, then the upper bound is readily available. Otherwise, when C is a polygon with n vertices, we can find $|C|$ with $\mathcal{O}(n)$ effort by for example triangulation. Also, $\text{diam}(C)$ can be found in $\mathcal{O}(n)$ using the idea of antipodal pairs and parallel support lines introduced by Shamos [52] or the idea of rotating calipers introduced in [53].

For the general convex set C we take one further step to bound the right hand side of (5.9) with something else to make the computation of the upper bound simpler. Let R_b be the minimum area axis-aligned bounding (enclosing) rectangle of C as shown in Figure 5.2. This can be obtained in $\mathcal{O}(T_x(C))$ time. Let p and q be the points where C touches the shorter sides of R_b . Let R' denote the minimum area rectangle enclosing C that has

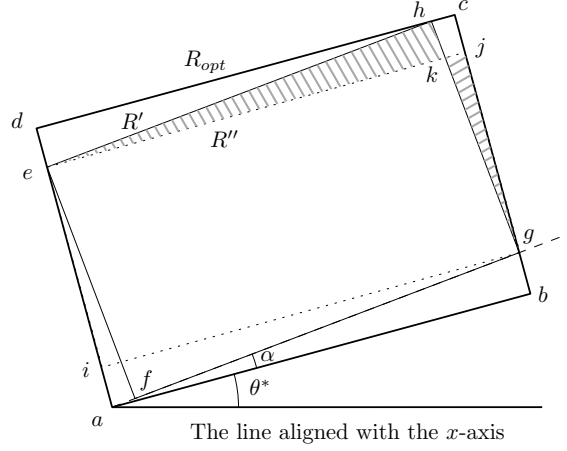


Figure 5.3: An illustration of the proof of the lower bound in Lemma 20. The rectangle R' is the largest rectangle with direction $\theta^* + \alpha$ inscribed in R_{opt} and the rectangle R'' is induced by R' .

a side parallel to the line segment \overline{pq} . Let $w' \geq |\overline{pq}|$ be the length of this side and h' the length of its other side. From Lemma 5 of Ahn et al. [34], we have $\text{diam}(C) \leq \sqrt{2}w'$ and $|C| \geq |R'|/(2\sqrt{2})$. Thus we have

$$\rho = \text{AR}(R_{opt}) \leq \frac{4(\text{diam}(C))^2}{|C|} \leq \frac{16\sqrt{2}(w')^2}{|R'|} \leq 16\sqrt{2} \text{AR}(R') \quad (5.10)$$

For a convex polygon, this weaker bound can be obtained in $\mathcal{O}(\log n)$. \square

Remark 4. The right hand side of (5.9) is minimized when C is a circle giving an upper bound of $16/\pi < 5.1$, while in that case we have $\text{AR}(R_{opt}) = 1$. The quality of this upper bound is not our goal here but we expect that this bound could be improved.

Lemma 20. *Let the optimal rectangle R_{opt} to have the aspect ratio ρ and the direction angle θ^* with the x -axis. Also, let $\bar{\rho}$ be the upper bound on ρ . Then, R_{apx} , the largest inscribed rectangle with direction angle $\theta_{apx} \in [\theta^* - \alpha, \theta^* + \alpha]$, for some small $\alpha > 0$, has area of at least $(1 - 2\bar{\rho}\alpha)|R_{opt}|$.*

Proof. First note that it suffices to consider only extreme points. For any non-extreme point $\theta' \in [\theta^* - \alpha, \theta^* + \alpha]$ there exists an α' with $0 < \alpha' < \alpha$ such that $\theta' = \theta^* - \alpha'$ or $\theta' = \theta^* + \alpha'$, i.e. θ' is one of the extreme points of $[\theta^* - \alpha', \theta^* + \alpha']$. Hence, we will have

$|R_{apx}| \geq (1 - 2\rho\alpha')|R_{opt}| \geq (1 - 2\rho\alpha)|R_{opt}|$. Also, it suffices to consider only one of the extreme cases, say $\theta^* + \alpha$, as the analysis for the other extreme case is symmetric. Now assume R_{apx} has direction angle $\theta^* + \alpha$, where R_{apx} is the largest inscribed rectangle for this direction and θ^* could be any angle in $[-\pi/4, \pi/4]$.

Consider Figure 5.3 as an illustration for the proof. Let rectangle $\square abcd$, in c.c.w. order, to represent R_{opt} and w.l.o.g. assume that $|\overline{ab}| \geq |\overline{bc}|$ (otherwise we can consider $\theta^* + \pi/2$ instead of θ^*) and that a is its lower left corner. Draw a line from a that makes the angle $\theta^* + \alpha$ with the x -axis. Let g be the intersection of this line with \overline{bc} . Let $R' = \square efgh$ be the largest rectangle with direction $\theta^* + \alpha$ inscribed in R_{opt} that has g as a corner. It is clear that $R' \subset R_{opt} \subset C$ and $|R_{apx}| \geq |R'|$, since R_{apx} is the largest rectangle with the direction angle $\theta^* + \alpha$ inscribed in $C \supseteq R_{opt}$. This can be also seen by Theorem 3 and the fact that f is in the interior of R_{opt} and there is no vertex-corner so there exists a larger rectangle with direction $\theta^* + \alpha$ inside R_{opt} that has four edge-corners and the area of that rectangle is also less than $|R_{apx}|$ by the previous argument.

Now, draw lines \overline{gi} and \overline{ej} parallel to \overline{ab} and let R'' to denote the rectangle $\square ejgi$. For small enough α the line segments \overline{ej} and \overline{gi} do not cross \overline{ag} and \overline{eh} . Also, let T_1, T_2 be the right triangles $\triangle ehk$ and $\triangle gjk$, respectively. We have $\alpha = \angle bag = \angle iga = \angle cgh = \angle dhe = \angle keh = \angle fea$, and $|\overline{ch}| \geq |\overline{jk}|$. Observe that $AR(R') \geq AR(R_{opt})$ and $|\overline{eh}| \geq |\overline{gh}|$. This gives

$$|\overline{cj}| = |\overline{de}| = |\overline{eh}| \sin \alpha \geq |\overline{gh}| \sin \alpha = |\overline{ch}|,$$

and

$$|\overline{cj}| = |\overline{de}| = |\overline{eh}| \sin \alpha \leq |\overline{ag}| \sin \alpha = |\overline{bg}|.$$

Thus we have

$$|T_2| = \frac{(|\overline{bc}| - |\overline{bg}| - |\overline{cj}|) \times |\overline{jk}|}{2} \leq \frac{(|\overline{bc}| - 2|\overline{cj}|) \times |\overline{ch}|}{2} = \frac{|\overline{bc}| \times |\overline{ch}| - 2|\overline{cj}| \times |\overline{ch}|}{2},$$

and

$$\begin{aligned}
|T_1| &= \frac{|\overline{ek}| \times |\overline{cj}|}{2} \geq \frac{|\overline{eh}| \times |\overline{cj}|}{2} \\
&= \frac{(|\overline{cd}| - |\overline{ch}|) \times |\overline{cj}|}{2 \cos \alpha} \\
&\geq \frac{|\overline{cd}| \times |\overline{cj}| - |\overline{cj}| \times |\overline{ch}|}{2} \\
&\geq \frac{(|\overline{bc}| - |\overline{cj}|) \times |\overline{ch}| - |\overline{cj}| \times |\overline{ch}|}{2} \\
&= \frac{|\overline{bc}| \times |\overline{ch}| - 2|\overline{cj}| \times |\overline{ch}|}{2}.
\end{aligned}$$

Hence, $|T_1| \geq |T_2|$ and therefore $|R'| \geq |R''|$. Using $|\overline{ab}| \leq \rho |\overline{bc}|$, we obtain a lower bound on the area of R'' as

$$\begin{aligned}
|R''| &= |\overline{eg}| \times |\overline{gj}| = |\overline{ab}| \times (|\overline{bc}| - |\overline{bg}| - |\overline{cj}|) \\
&\geq |\overline{ab}| \times (|\overline{bc}| - 2|\overline{bg}|) \\
&= |\overline{ab}| \times |\overline{bc}| - 2|\overline{ab}| \times |\overline{bg}| \\
&= |\overline{ab}| \times |\overline{bc}| - 2|\overline{ab}|^2 \tan \alpha \\
&\geq (|\overline{ab}| \times |\overline{bc}|) - 2\rho \tan \alpha (|\overline{ab}| \times |\overline{bc}|) \\
&\simeq (1 - 2\rho \alpha) |R_{opt}|.
\end{aligned}$$

Note that for sufficiently small α we have $\alpha \sim \tan \alpha$. Therefore, we obtain

$$|R_{apx}| \geq |R'| \geq |R''| \geq (1 - 2\rho \alpha) |R_{opt}| \geq (1 - 2\bar{\rho} \alpha) |R_{opt}|,$$

which concludes the proof. □

It remains to find a direction angle that is within the interval $[\theta^* - \alpha, \theta^* + \alpha]$.

Theorem 21. *Given a compact convex set $C \subset \mathbb{R}^2$, an ε -approximation solution for the problem of finding the maximum area inscribed rectangle (MAIR) in C can be obtained in $\mathcal{O}(\varepsilon^{-1} n \sqrt{n} (\log n + 2L))$ time.*

Proof. For any given $\varepsilon > 0$ take $\alpha > 0$ small enough such that $\varepsilon = 2\bar{\rho}\alpha$. We divide the interval $[-\frac{\pi}{4}, \frac{\pi}{4}]$ into $\frac{\pi/2}{\alpha} = \frac{\pi/2}{\varepsilon/(2\bar{\rho})} = \frac{\bar{\rho}\pi}{\varepsilon}$ pieces and sample one direction point from each piece. Finding $\bar{\rho}$ requires an $\mathcal{O}(T_x(C))$ pre-processing time; for convex polygons this can be computed in $\mathcal{O}(\log n)$, as shown in Lemma 19. Since the Problem (5.8) is solvable for any fixed t , then $\psi(t)$ is defined for all $t \in [-1, 1]$. We solve the exact subroutine of §5.2 for each sampled direction, and choose the maximum value of $f(t)$ over all these samples of t . The result will have an area of at least $(1 - \varepsilon)|R_{opt}|$ by Lemma 20. Considering the complexity of the exact subroutine, the computational complexity of this algorithm is $\mathcal{O}(\frac{\bar{\rho}\pi}{\varepsilon}n\sqrt{n}(\log n + 2L)) = \mathcal{O}(\varepsilon^{-1}n\sqrt{n}(\log n + 2L))$. \square

A Family of Approximation Algorithms for Finding the MAIR Inside a Convex Polygon

When C is a convex polygon, the parametrized optimization approach is not restricted to use the exact subroutine presented in Section 5.2 and any of the existing efficient algorithms from the literature that can find the MAAIR in a convex polygon can be used as a subroutine. The following theorem states the results for the case when the best-known algorithm for finding the MAAIR in convex polygons is used as the subroutine to the parametrized optimization algorithm.

Theorem 22. *Give a compact convex polygon P , an ε -approximation solution for the problem of finding the maximum area inscribed rectangle (MAIR) in P can be obtained in $\mathcal{O}(\varepsilon^{-1} \log n)$ time with an $\mathcal{O}(\varepsilon^{-1}n)$ pre-processing time.*

Proof. Replace the exact subroutine of Section 5.2 with the algorithm from Alt et al. [30] that takes $\mathcal{O}(\log n)$ to find the MAAIR in a convex polygon for any of the $\mathcal{O}(\varepsilon^{-1})$ directions. By Lemma 19, finding $\bar{\rho}$ requires an $\mathcal{O}(\log n)$ pre-processing time. Also, the rotation of the axes and finding the new coordinates for n vertices of P takes an $\mathcal{O}(n)$ pre-processing time for each of the $\mathcal{O}(\varepsilon^{-1})$ directions. \square

Chapter 6

Computational Experiments

6.1 Simulation Results

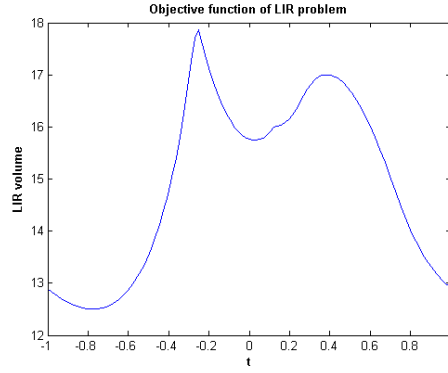
Here we apply the presented algorithms on convex sets such as polygons, ellipses, and the bounded intersection of convex sets. Simulation results for two given polygons and two random polygons are shown in Figure 6.1 and Figure 6.2, respectively. Examples of axis-aligned rectangles for the regular and rotated axes are shown in Figure 6.3. Examples for ellipses and for the intersection of some convex sets are shown in Figures 6.4 and 6.5, respectively.

6.2 Evaluation

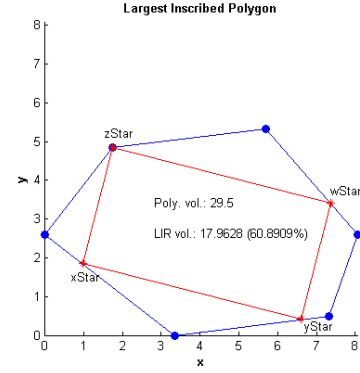
This thesis considered both problems of finding MVAIR (MAAIR) and MVIR (MAIR) inside a convex set. Unlike most of the literature, that considers this set to be a polygon (a set of linear inequalities), this thesis relaxes this set to be any geometric convex body that is expressible in a finite number of convex inequalities. Such convex sets include polytopes (polygons), ellipsoids, and the intersection of convex sets such as the intersection of ellipses and halfspaces or the bounded intersection of the epigraph of convex parabolas with ellipses and halfspaces. The MVIR problem is formulated as a non-convex optimization problem, while a convex optimization problem is developed for the MVAIR problem, both models

in higher dimensions. The models can also be easily generalized to the cases of finding other inscribed geometric shapes. The proposed algorithm finds an ε -approximation to the MVAIR in a convex set in $\mathcal{O}((d^3 + d^2n)\sqrt{n} \log \frac{n}{\varepsilon})$ time, where d is the dimension, n is the number of inequalities defining the convex set. This can be rounded to optimality in a polynomial number of elementary operations in terms of d by choosing a small enough ε . For finding MAIR in a 2D convex set, a parametric approach is developed that helps us to find the optimal MAIR in any given direction of axes, which can be used as a subroutine to compute $(1 - \varepsilon)$ -approximation to MAIR in $\mathcal{O}(\varepsilon^{-1}n\sqrt{n}(\log n + 2L))$ time, where L is the size of the problem defined as the binary input length of the problem, i.e., the number of bits needed to encode the problem. When the convex set is a polygon the running time can be improved to $\mathcal{O}(\varepsilon^{-1} \log n)$. For the special case of convex polygons our algorithm works faster than Knauer et al.'s algorithm [32] and in cases where a highly accurate solution for practical size polygons is needed, it also outperforms Cabello et al.'s algorithm [33].

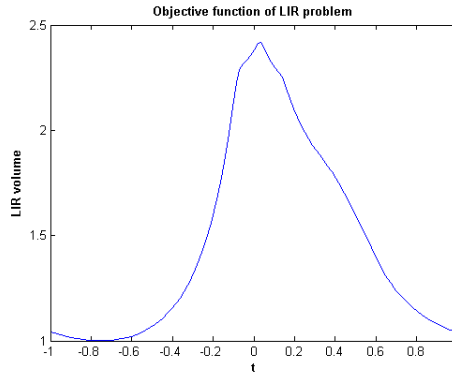
To our knowledge, except Amenta's model [26] for the MVAIR problem and the model of Cabello et al. [33] for the MAIR problem, no other optimization-based algorithm published so far for these two problems. Furthermore, except for Amenta's model for MVAIR [26], we are not aware of any model or algorithm for the higher dimension problem. Our optimization model for the MVAIR problem is much more efficient than Amenta's model as it reduces the $\mathcal{O}(n2^d)$ number of constraints to $\mathcal{O}(n)$ constraints. While none of the existing algorithms can solve both general and axis-aligned problems, our parametric approach can do so in 2D. Moreover, except Cabello et al.'s algorithm [33], no algorithm is published so far for either of these problems capable of dealing with a broader spectrum of geometric convex sets other than polygons. The dependence of the running time of Cabello et al.'s algorithm [33] to unknown factor T_C makes it difficult to compare it with our algorithms for the general convex sets described by convex inequalities. Our algorithm is unique regarding the dependence of its performance on the number of inequalities defining the convex set; although for a polygon, this is n , for an ellipse, this is just one.



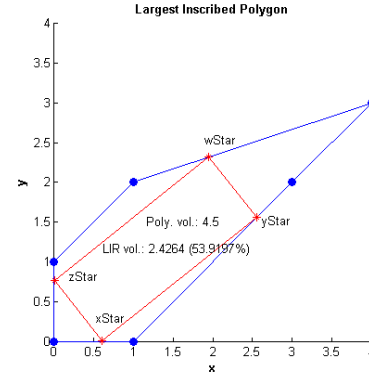
(a)



(b)



(c)



(d)

Figure 6.1: The largest inscribed rectangle in two given polygons. The objective functions are shown in (6.1a) and (6.1c). It can be seen that $f(-1) = f(1)$ but $f(t)$ is not necessarily symmetric or even unimodal over $-1 \leq t \leq 1$. The largest inscribed rectangles are obtained in (6.1b) and (6.1d), using the algorithm described in Section 5.2. “Poly. vol.” shows the area (volume in general) of the polygon and “LIR vol.” show the area of the largest inscribed rectangle and the percentage of this area to the area of the polygon. Figure (6.1b) shows the MAIR with one vertex-corner and three edge-corners, while the MAIR in Figure (6.1d) has four edge-corners.

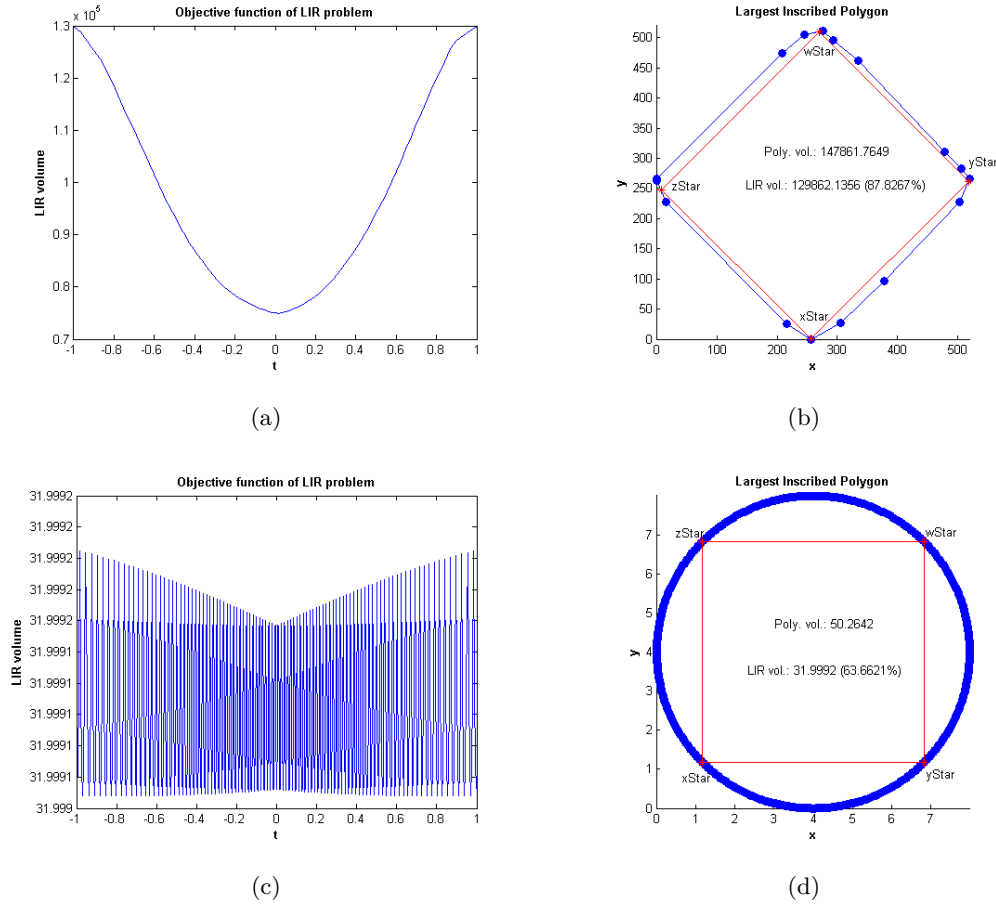
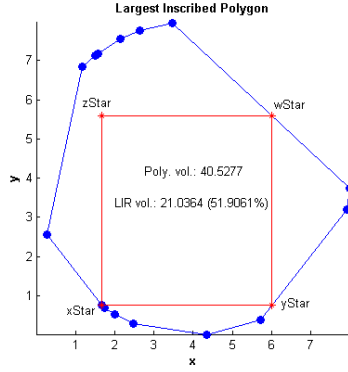
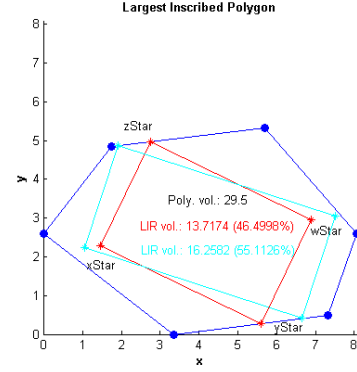


Figure 6.2: The largest inscribed rectangle in a random polygon with 14 vertices and a regular 500-gon randomly generated on a circle. The objective functions are shown in (6.2a) and (6.2c), which shows the contrast between a well-behaved unimodal quasiconvex and almost symmetric function and an ill-behaved non-smooth function. The largest inscribed rectangles are obtained in (6.2b) and (6.2d). It should be noted that the largest inscribed rectangle inside a circle is a square and the fraction of the area at optimality is $2/\pi \simeq 0.63662$.

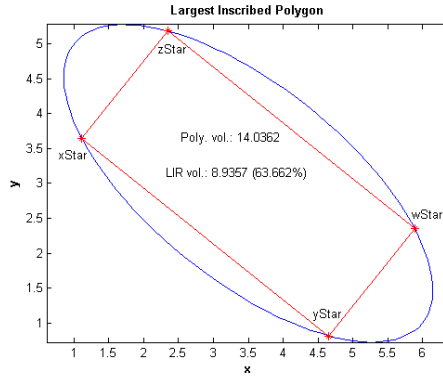


(a)

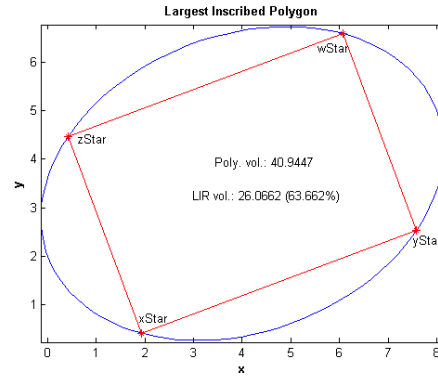


(b)

Figure 6.3: The maximum area axis-aligned inscribe rectangles for the regular axes in a random 15-gon generated on a circle in (6.3a) and for two given directions in a given polygon in (6.3b). Note in Figure (6.3b) that the conditions of Theorem 3 may not hold for the maximum area rectangles for given directions as they may not be optimal regarding all directions.

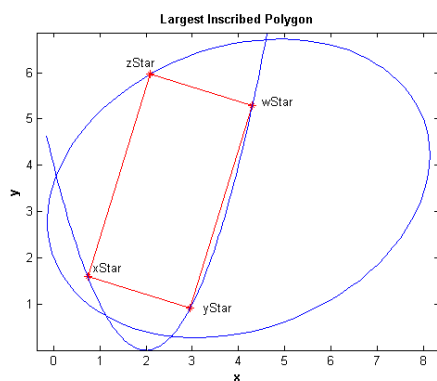


(a)

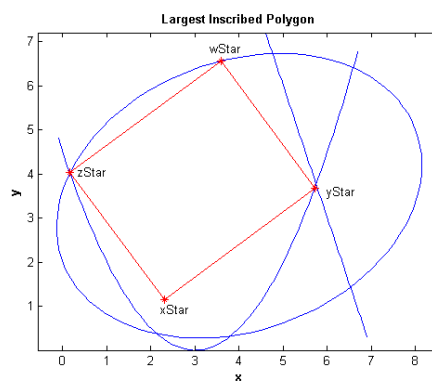


(b)

Figure 6.4: The largest inscribed rectangles in two given ellipses. Notably, the fraction of the area of the MAIR to the area of the ellipse is the same as that of circles ($2/\pi \simeq 0.63662$), which can be verified by the elementary calculus.



(a)



(b)

Figure 6.5: The largest inscribed rectangle in the intersection of an ellipse and a parabola is presented in (6.5a) and for the intersection of an ellipse, a parabola, and a half-space is shown in (6.5b). We see that the conditions of the Theorem 3 hold for these particular non-polygonal examples.

Chapter 7

Conclusion

We have presented several optimization models for the problem of finding the maximum volume (axis-aligned) inscribed rectangle in a convex set defined by a finite number of convex inequalities. We presented efficient exact and $(1-\varepsilon)$ -approximation algorithms for the MVAIR, MAAIR, and MAIR problems. The running time of these algorithms only depends on the dimension and the number of convex inequalities that define the convex set. We have also analyzed the optimal properties of the MAIR in convex polygons, centrally symmetric convex sets, and axially symmetric convex sets. One future research direction is to explore the optimal properties of the MVIR problem in the higher dimension and use those properties in developing efficient algorithms for finding the MVIR. Another potential direction for future research would be the consideration of inscribing other geometric shapes in a convex set or approximating a convex set that contains “holes” with multiple inscribed rectangles. One could also consider extending the existing results of similar shape approximation problems to higher dimensions.

Bibliography

- [1] Fritz John. Extremum problems with inequalities as subsidiary conditions, studies and essays presented to r. courant on his 60th birthday, january 8, 1948, 1948.
- [2] Fritz John. Extremum problems with inequalities as subsidiary conditions. In *Traces and emergence of nonlinear programming*, pages 197–215. Springer, 2014.
- [3] Martin Henk. Löwner-John Ellipsoids. *Documenta Math*, pages 95–106, 2012.
- [4] George Pólya and Gabriel Szegő. *Isoperimetric inequalities in mathematical physics*. Number 27. Princeton University Press, 1951.
- [5] Victor Milenkovic, Karen Daniels, and Zhenyu Li. Automatic marker making. In *Proceedings of the Third Canadian Conference on Computational Geometry*, pages 243–246. Simon Fraser University, 1991.
- [6] Victor J Milenkovic, Karen Daniels, and Zhenyu Li. Placement and compaction of nonconvex polygons for clothing manufacture. In *In Proceedings of the 4th Canadian Conference on Computational Geometry*. Citeseer, 1992.
- [7] Karen L Daniels, Victor Milenkovic, and Dan Roth. Finding the maximum area axis-parallel rectangle in a polygon. In *CCCG*, pages 322–327. Citeseer, 1993.
- [8] A DePano, Yah Ke, and J O’Rourke. Finding largest inscribed equilateral triangles and squares. In *Proc. 25th Allerton Conf. Commun. Control Comput*, pages 869–878, 1987.

-
- [9] Helmut Alt, Johannes Blömer, and Hubert Wagener. Approximation of convex polygons. In *International Colloquium on Automata, Languages, and Programming*, pages 703–716. Springer, 1990.
 - [10] Binhai Zhu. Approximating convex polyhedra with axis-parallel boxes. *International Journal of Computational Geometry & Applications*, 7(03):253–267, 1997.
 - [11] Jeet Chaudhuri, Subhas C Nandy, and Sandip Das. Largest empty rectangle among a point set. *Journal of algorithms*, 46(1):54–78, 2003.
 - [12] Kai Jin. Finding all maximal area parallelograms in a convex polygon. *arXiv preprint arXiv:1711.00181*, 2017.
 - [13] Kai Jin. Maximal parallelograms in convex polygons and a novel geometric structure. *arXiv preprint arXiv:1512.03897*, 2018.
 - [14] Vahideh Keikha, Maarten Löffler, Ali Mohades, Jérôme Urhausen, and Ivor van der Hoog. Maximum-area triangle in a convex polygon, revisited. *arXiv preprint arXiv:1705.11035*, 2017.
 - [15] David P Dobkin and Lawrence Snyder. On a general method for maximizing and minimizing among certain geometric problems. In *20th Annual Symposium on Foundations of Computer Science (sfcs 1979)*, pages 9–17. IEEE, 1979.
 - [16] Sharat Chandran and David M Mount. A parallel algorithm for enclosed and enclosing triangles. *International Journal of Computational Geometry & Applications*, 2(02):191–214, 1992.
 - [17] Yoav Kallus. A linear-time algorithm for the maximum-area inscribed triangle in a convex polygon. *arXiv preprint arXiv:1706.03049*, 2017.
 - [18] Kai Jin. Maximal area triangles in a convex polygon. *arXiv preprint arXiv:1707.04071*, 2018.

-
- [19] Konstanty Radziszewski. Sur un probleme extrémal relatif aux figures inscrites et circonscrites aux figures convexes. *Ann. Univ. Mariae Curie-Sklodowska, Sect. A*, 6:5–18, 1952.
 - [20] Hugo Hadwiger. Volumschätzung für die einen Eikörper überdeckenden und unterdeckenden Parallelotope. *Elemente der Mathematik*, 10:122–124, 1955.
 - [21] A Kosiński. A proof of an Auerbach-Banach-Mazur-Ulam theorem on convex bodies. In *Colloquium Mathematicae*, volume 4, pages 216–218. Institute of Mathematics Polish Academy of Sciences, 1957.
 - [22] Branko Grünbaum. Measures of symmetry for convex sets. In *Convexity: Proceedings of the Seventh Symposium in Pure Mathematics of the American Mathematical Society*, volume 7, pages 233–270. American Mathematical Soc., 1963.
 - [23] Marek Lassak. Approximation of convex bodies by rectangles. *Geometriae Dedicata*, 47(1):111–117, 1993.
 - [24] Otfried Schwarzkopf, Ulrich Fuchs, Günter Rote, and Emo Welzl. Approximation of convex figures by pairs of rectangles. *Computational Geometry*, 10(2):77–87, 1998.
 - [25] Jan Brinkhuis. Inner and outer approximation of convex sets using alignment. *Optimization Letters*, 10(7):1403–1416, 2016.
 - [26] Nina Amenta. Bounded boxes, Hausdorff distance, and a new proof of an interesting Helly-type theorem. In *Proceedings of the tenth annual symposium on Computational geometry*, pages 340–347. ACM, 1994.
 - [27] Karen Daniels, Victor Milenkovic, and Dan Roth. Finding the largest area axis-parallel rectangle in a polygon. *Computational Geometry*, 7(1):125–148, 1997.
 - [28] Wilhelm Ackermann. Zum hilbertschen aufbau der reellen zahlen. *Mathematische Annalen*, 99(1):118–133, 1928.

-
- [29] Paul Fischer and Klaus-Uwe Höffgen. Computing a maximum axis-aligned rectangle in a convex polygon. *Information Processing Letters*, 51(4):189–193, 1994.
- [30] Helmut Alt, David Hsu, and Jack Snoeyink. Computing the largest inscribed isothetic rectangle. In *CCCG*, pages 67–72, 1995.
- [31] Olaf Hall-Holt, Matthew J Kate, Piyush Kumar, and Joseph SB Mitchell. Finding large sticks and potatoes in polygons. In *Proceedings of the Seventeenth Annual ACM-SIAM Symposium on Discrete Algorithms*, volume 122, page 474. SIAM, 2006.
- [32] Christian Knauer, Lena Schlipf, Jens M Schmidt, and Hans Raj Tiwary. Largest inscribed rectangles in convex polygons. *Journal of Discrete Algorithms*, 13:78–85, 2012.
- [33] Sergio Cabello, Otfried Cheong, Christian Knauer, and Lena Schlipf. Finding largest rectangles in convex polygons. *Computational Geometry*, 51:67–74, 2016.
- [34] Hee-Kap Ahn, Peter Brass, Otfried Cheong, Hyeon-Suk Na, Chan-Su Shin, and Antoine Vigneron. Inscribing an axially symmetric polygon and other approximation algorithms for planar convex sets. *Computational Geometry*, 33(3):152–164, 2006.
- [35] Lena Marie Schlipf. *Stabbing and Covering Geometric Objects in the Plane*. PhD thesis, 2014.
- [36] Stephen Boyd and Lieven Vandenbergh. *Convex optimization*. Cambridge university press, 2004.
- [37] Yu E Nesterov. Polynomial time methods in linear and quadratic programming. *Izvestija AN SSR, Tekhnicheskaya kibernetika*, (3):324–326, 1988. (In Russian).
- [38] Yu E Nesterov. Polynomial time iterative methods in linear and quadratic programming. *Voprosy kibernetiki, Moscow*, pages 102–125, 1988. (In Russian).
- [39] Yurii Nesterov and Arkadi Nemirovsky. Polynomial-time barrier methods in convex programming. *Ekonomika i Matem. Metody*, 24(7):1084–1091, 1988. (In Russian; English trans. Matekon: Translations of Russian and East European Math. Economics.).

-
- [40] Yu E Nesterov and A Nemirovsky. Self-concordant functions and polynomial-time methods in convex programming. *Report, Central Economic and Mathematic Institute, USSR Acad. Sci*, 1989.
 - [41] Yurii Nesterov and Arkadi Nemirovsky. Acceleration and parallelization of the path-following interior point method for a linearly constrained convex quadratic problem. *SIAM Journal on Optimization*, 1(4):548–564, 1991.
 - [42] Yurii Nesterov and Arkadii Nemirovskii. *Interior-point polynomial algorithms in convex programming*. SIAM, 1994.
 - [43] Arkadi S Nemirovski and Michael J Todd. Interior-point methods for optimization. *Acta Numerica*, 17(1):191–234, 2008.
 - [44] Arkadi Nemirovski. Lecture notes: Interior point polynomial time methods in convex programming. *Spring Semester*, 2004.
 - [45] H Minkowski. Allgemeine lehätze über konvexe polyeder. *Ges. Abh., Leipzog-Berlin*, 1:103–121, 1911.
 - [46] Dimitris Bertsimas and John N Tsitsiklis. *Introduction to linear optimization*, volume 6. Athena Scientific Belmont, MA, 1997.
 - [47] Miguel Sousa Lobo, Lieven Vandenbergh, Stephen Boyd, and Hervé Lebret. Applications of second-order cone programming. *Linear algebra and its applications*, 284(1-3):193–228, 1998.
 - [48] Christos H Papadimitriou and Kenneth Steiglitz. *Combinatorial optimization: algorithms and complexity*. Courier Corporation, 1998.
 - [49] Dirk Den Hertog. *Interior point approach to linear, quadratic and convex programming: algorithms and complexity*, volume 277. Springer Science & Business Media, 2012.
 - [50] Anthony V Fiacco and Yo Ishizuka. Sensitivity and stability analysis for nonlinear programming. *Annals of Operations Research*, 27(1):215–235, 1990.

-
- [51] Georg Still. Lectures on parametric optimization: An introduction.
 - [52] Michael Ian Shamos. Computational geometry. *Ph. D. thesis, Yale University*, 1978.
 - [53] Godfried T Toussaint. Solving geometric problems with the rotating calipers. In *Proc. IEEE Melecon*, volume 83, page A10, 1983.